Constraining supernova neutrino detection with weak decay available data

Arturo R. Samana

in collaboration with
Francisco Krmpotic, Alejandro Mariano, Cesar Barbero – UNLP -Argentina
Carlos A. Bertulani -Texas A&M University – Commerce-USA
Nils Paar – University of Zagreb – Croatia

08/15/2016

INT-16-61W– Seattle- USA - 2016

Outline

- Motivation

- On neutrino physics and nuclear structure.

- Detection of supernovae neutrinos

- Weak-Nuclear interaction formalism
- Nuclear Models

  QRPA & RQRPA

- Some numerical results

  $\nu_e / \bar{\nu}_e$ 56Fe and 40Ar cross section

- Summary

Motivation

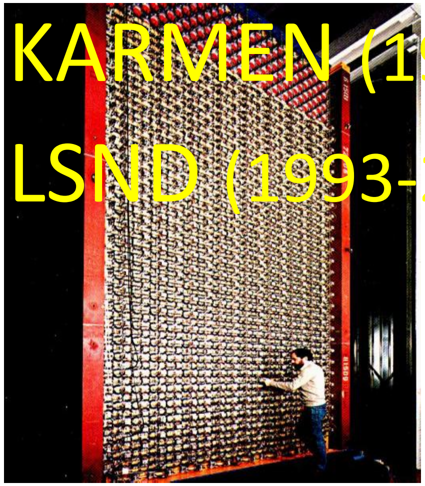

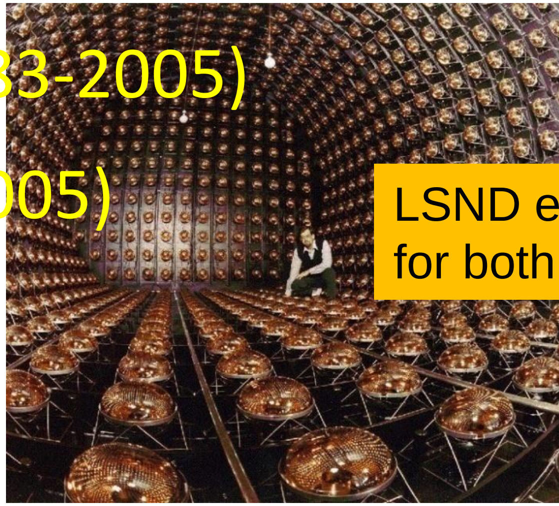

KARMEN (1983-2005)

LSND (1993-2005)

KARMEN, no oscillation signal

LSND experiment observes excesses of events for both the $\bar{\nu}_\mu \rightarrow \bar{\nu}_e$ and $\nu_\mu \rightarrow \nu_e$ oscillation.

$$\bar{\sigma}(J_f) = \int n(E_\nu)\sigma(E_\nu, J_f)dE_\nu$$

Table 1

Calculated and experimental flux-averaged exclusive $\bar{\sigma}^{exc}_{e,\mu}$, and inclusive $\bar{\sigma}^{inc}_{\mu}$ cross-section for the $^{12}C(\nu_e, e^-)^{12}N$ DAR reaction (in units of 10^{-42} cm^2) and for the $^{12}C(\nu_\mu, \mu^-)^{12}N$ DIF reaction (in units of 10^{-40} cm^2). The CRPA calculations [15] were used in the first LSND analysis on the 1993–1995 data sample [2], and the SM calculations from Ref. [16] in the second LSND oscillation search [3]. The listed PQRPA results correspond to the calculations performed with the relativistic corrections included [17]. One alternative SM result as well as the RPA and QRPA results from Ref. [19] are also shown

	$\bar{\sigma}^{exc}_{e}$	$\bar{\sigma}^{inc}_{e}$	$\bar{\sigma}^{exc}_{\mu}$	$\bar{\sigma}^{inc}_{\mu}$
Theory				
CRPA [15]	36.0, 38.4	42.3, 44.3	2.48, 3.11	21.1, 22.8
SM [16]	7.9	12.0	0.56	13.8
PQRPA [17]	8.1	18.6	0.59	13.0
SM [19]	8.4	16.4	0.70	21.1
RPA [19]	49.5	55.1	2.09	19.2
QRPA [19]	42.9	52.0	1.97	20.3
Experiment				
Ref. [20]	$9.1 \pm 0.4 \pm 0.9$	$14.8 \pm 0.7 \pm 1.4$		
Ref. [21]			$0.66 \pm 0.1 \pm 0.1$	$12.4 \pm 0.3 \pm 1.8$
Ref. [22]	$8.9 \pm 0.3 \pm 0.9$	$13.2 \pm 0.4 \pm 0.6$		
Ref. [23]			$0.56 \pm 0.08 \pm 0.10$	$10.6 \pm 0.3 \pm 1.8$

A. Samana , F. Krmpotic , A. Mariano,R. Zukanovich Funchal/ Phys. Lett B642(2006)100

Motivation

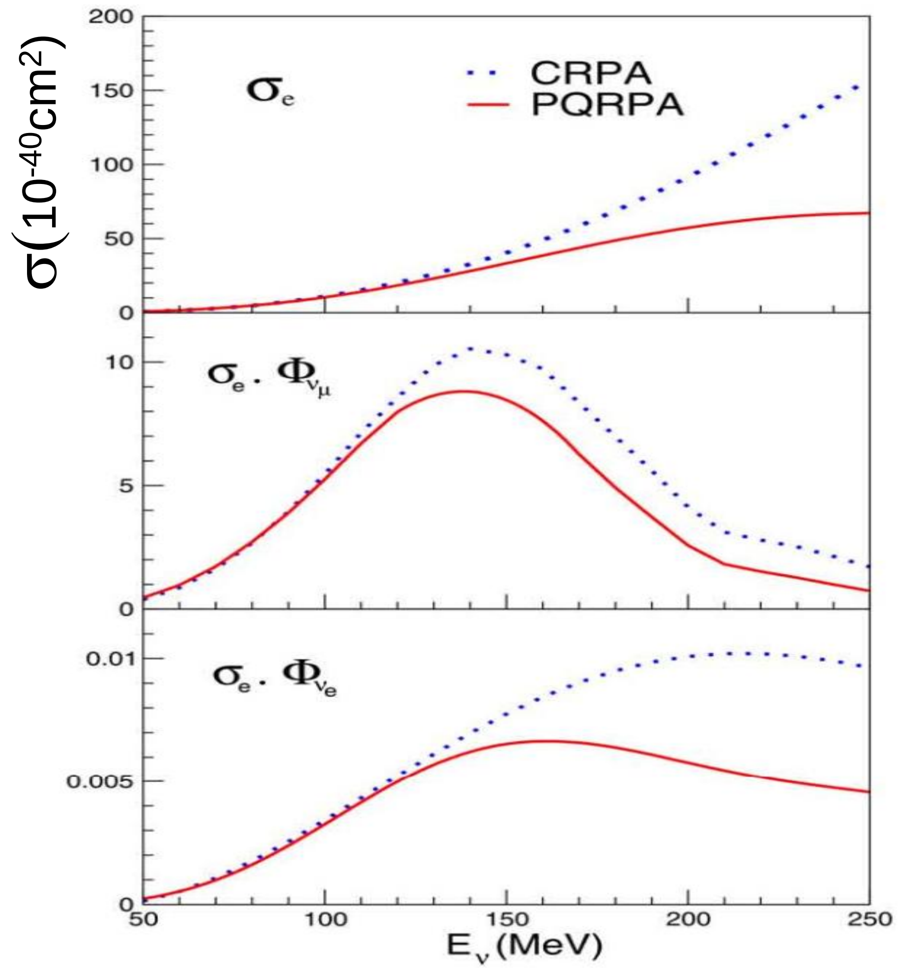

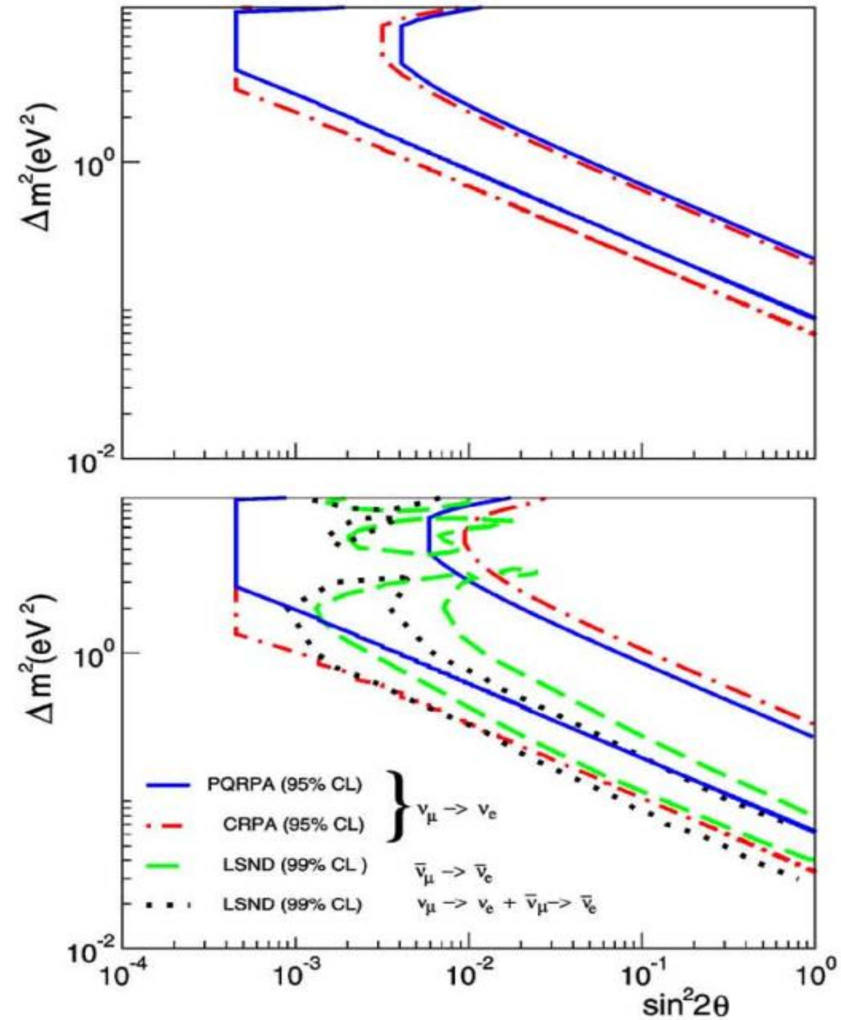

ν-nucleus cross section are important to constrain parameters in neutrino oscillations.

$\overline{\nu}_\mu \rightarrow \overline{\nu}_e \qquad \nu_\mu \rightarrow \nu_e$

* Increase probability oscillations.
* Confidence level region is diminished by difference in σ_e between PQRPA and CRPA, PLB (2005) 100

Supernovae Neutrinos – Signal Detection

Number of target nuclei

Neutrino flux

Interaction cross section

Efficiency

$$N_{ev} = N_t \int_0^{\infty} F(E_\nu)\cdot\sigma(E_\nu)\cdot\varepsilon(E_\nu)\,dE_\nu$$

$$\sigma(E_\nu) \Updownarrow F(E_\nu)$$

SNO

$$\nu_e + d \rightarrow p + p + e^-$$

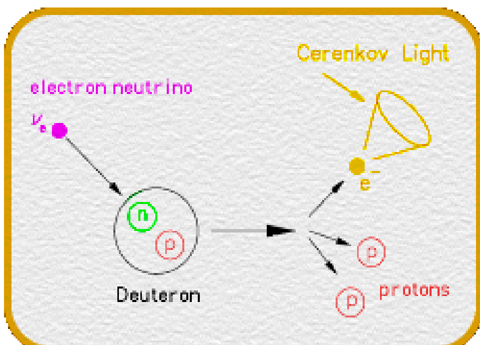

$$\bar{\nu}_e + p \rightarrow n + e^+$$

Super-K

$$\nu_e + {}^{16}O \rightarrow {}^{16}F + e^-$$

$$\bar{\nu}_e + {}^{16}O \rightarrow {}^{16}N + e^+$$

LVD

$$\nu_e + {}^{12}C \rightarrow {}^{12}N + e^-$$

$$\bar{\nu}_e + {}^{12}C \rightarrow {}^{12}B + e^+$$

$$\nu_e + {}^{56}Fe \rightarrow {}^{56}Co + e^-$$

$$\bar{\nu}_e + {}^{56}Fe \rightarrow {}^{56}Mn + e^+$$

Supernovae Neutrinos – Signal Detection

LArTPC - Liquid **Ar**gon **T**ime **P**rojection **C**hambers: ν-40 Ar

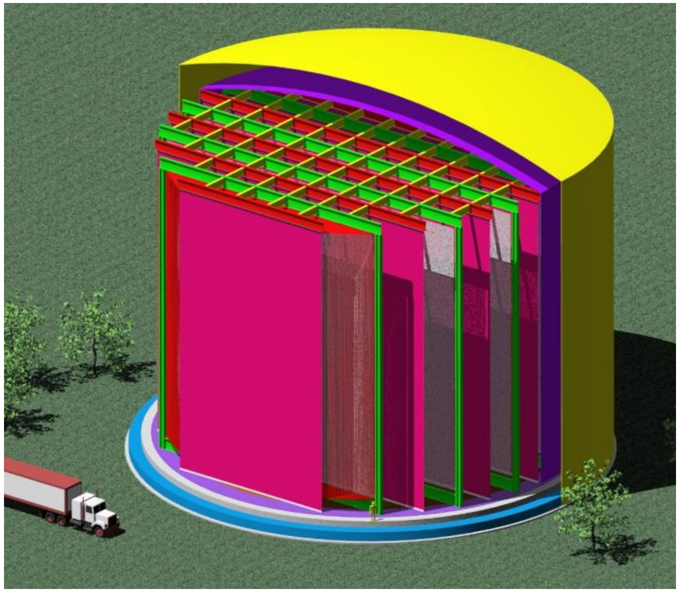

http://www-lartpc.fnal.gov/

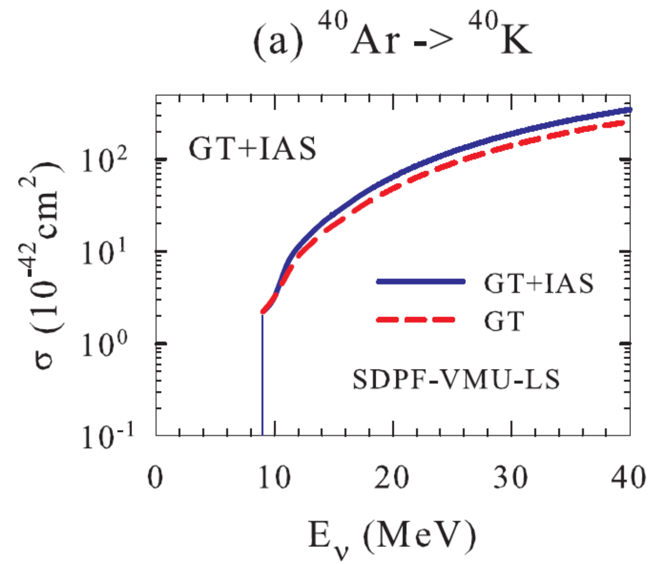

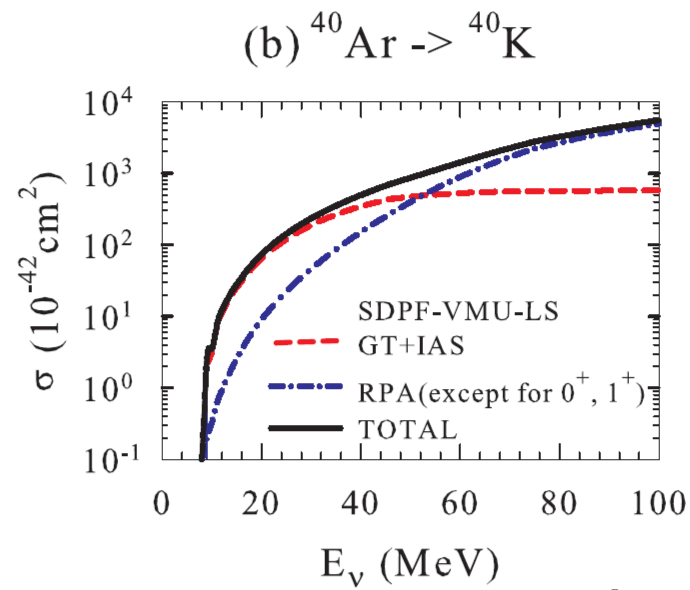

RPA: Martinez-Pinedo, Kolbe & Langanke K, priv. comm. in Gil-Botella & Rubbia, JCAP10 (2003) 009
SM : T. Suzuki & M. Honma, arXiv:1211.4078v1 [nucl-th] 17 Nov 2012
QRPA : M. Cheoun etal , Phys. Rev. **C 83,** 028801 (2011)
PQRPA: actual calculations

Weak–nuclear interaction

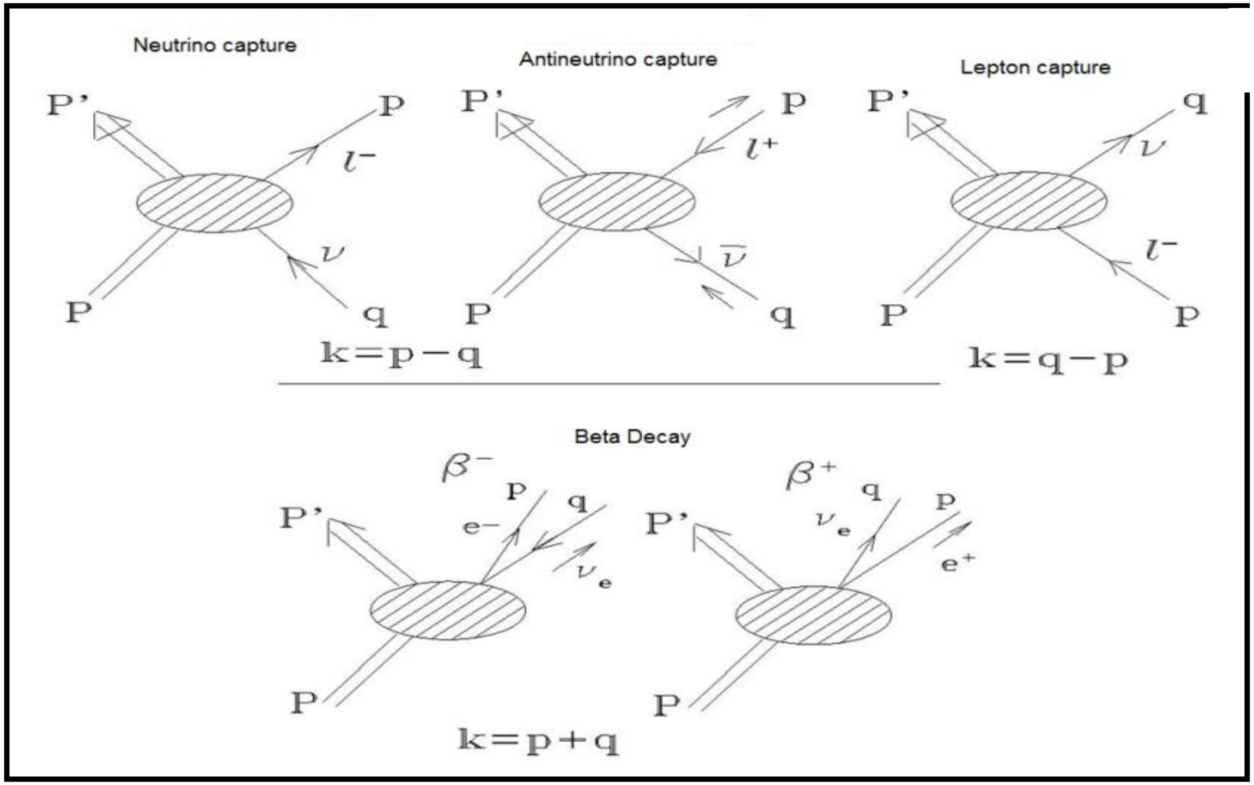

Charged Current

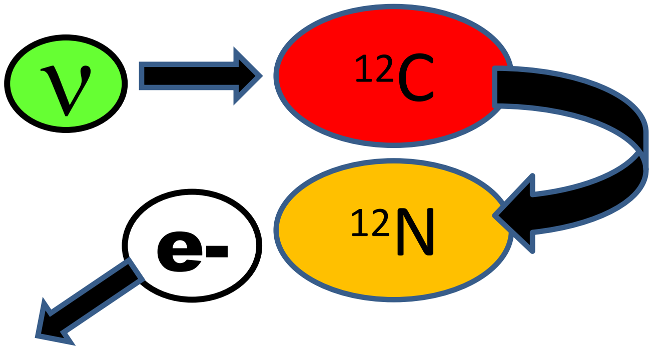

Neutral Current

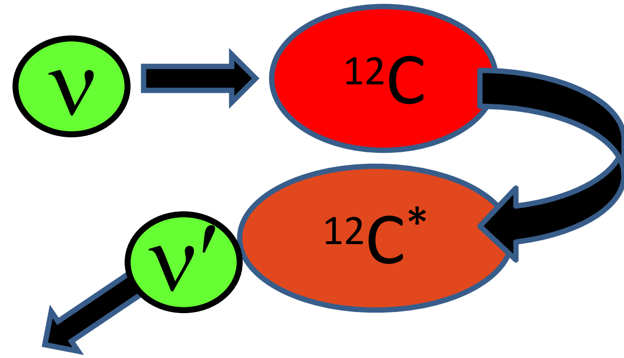

$$\nu_e + A(Z,N) \Rightarrow A^*(Z+1,N-1) + e^-$$

$$\bar{\nu}_e + A(Z,N) \Rightarrow A^*(Z-1,N+1) + e^+$$

(i)O'Connell, Donelly & Walecka, PR6,719 (1972)
(ii) Kuramoto etal. NPA 512, 711 (1990)
(iii) Luyten etal. NP41,236 (1963)
(iv) Krmpotic etal. PRC71, 044319(2005).

ALL ARE EQUIVALENTS.

Weak–nuclear interaction

Reaction:

$$\nu_l + (Z, A) \rightarrow (Z+1, A) + l^-$$

Weak hamiltonian:

$$H_W(\vec{r}) = \frac{G}{\sqrt{2}} J_\alpha l_\alpha e^{-i\vec{k}\cdot\vec{r}}$$

$$J_\alpha = i\gamma_4\left[g_V\gamma_\alpha - \frac{g_M}{2\mathrm{M}}\sigma_{\alpha\beta}k_\beta + g_A\gamma_\alpha\gamma_5 + i\frac{g_P}{\mathrm{m}_\ell}k_\alpha\gamma_5\right]$$

$$l_\alpha = -i\overline{u}_{s_\ell}(\mathbf{p}, E_\ell)\gamma_\alpha(1+\gamma_5)u_{s_\nu}(\mathbf{q}, E_\nu)$$

Neutrino-nucleus cross section (Fermi's Golden Rule):

$$\sigma(E_l, J_f) = \frac{p_l E_l}{2\pi} F(Z+1, E_l) \int_{-1}^{1} d(\cos\theta) T_\sigma(|\vec{k}|, J_f)$$

p_l :Lepton momentum, E_l: Lepton energy, *F(Z+1,E):* Fermi function

Transition amplitude

$$\mathrm{T}_\sigma(|\vec{k}|, J_f) \equiv \frac{1}{2J_i+1}\sum_{s_l s_\nu}\sum_{M_f M_i}\left|\left\langle J_f M_f \,|\, H_W \,|\, J_i M_i\right\rangle\right|^2 = \frac{G^2}{2J_i+1}\sum_{M_f M_i}\mathrm{O}_\alpha \mathrm{O}^*_\beta L_{\alpha\beta}$$

$\mathrm{O}_\alpha = \left\langle J_f \,||\, J_\alpha e^{-i\vec{k}\cdot\vec{r}} \,||\, J_i\right\rangle,$ Nuclear Matrix Element , Lepton traces $L_{\alpha\beta}$

$k = (\vec{k}, k_\varnothing), \rho = \kappa.r = |\vec{k}|.r$ Transfer momentum, with **k**= |**k**| ž.

Weak–nuclear interaction

Non-relativistic approximation of hadronic current

$$J_\emptyset = g_V + (\overline{g}_A + \overline{g}_{P1})\boldsymbol{\sigma}\cdot\hat{\mathbf{k}} + ig_A M^{-1}\boldsymbol{\sigma}\cdot\boldsymbol{\nabla},$$

$$\mathbf{J} = -g_A\boldsymbol{\sigma} - i\overline{g}_W\boldsymbol{\sigma}\times\hat{\mathbf{k}} - \overline{g}_V\hat{\mathbf{k}} + \overline{g}_{P2}(\boldsymbol{\sigma}\cdot\hat{\mathbf{k}})\hat{\mathbf{k}} - ig_V M^{-1}\boldsymbol{\nabla},$$

Nuclear coupling constant

$$g_V = 1, \quad g_A = 1.26, \longrightarrow \boxed{g_A \sim 1}$$

$$g_M = \kappa_p - \kappa_n = 3.70, \quad g_P = g_A\frac{2\mathrm{M}\mathrm{m}_\ell}{k^2 + \mathrm{m}_\pi^2}.$$

FNS effect: $g \rightarrow g\left(\frac{\Lambda^2}{\Lambda^2 + k^2}\right)^2$

Λ=850 MeV

Transfer momentum, with **k**= |**k**| ž.

$$e^{-i\mathbf{k}\cdot\mathbf{r}} = \sum_L i^{-L}\sqrt{4\pi(2L+1)}\, j_L(\kappa r) Y_{L0}(\hat{\mathbf{r}}),$$

Elementary Operators :

$$\mathcal{M}_J^V = j_J(\rho)Y_J(\hat{\mathbf{r}}),$$
$$\mathcal{M}_J^A = \kappa^{-1} j_J(\rho)Y_J(\hat{\mathbf{r}})(\boldsymbol{\sigma}\cdot\boldsymbol{\nabla}),$$
$$\mathcal{M}_{MJ}^A = \sum_L i^{J-L-1} F_{MLJ}\, j_L(\rho)\left[Y_L(\hat{\mathbf{r}})\otimes\boldsymbol{\sigma}\right]_J,$$
$$\mathcal{M}_{MJ}^V = \kappa^{-1}\sum_L i^{J-L-1} F_{MLJ}\, j_L(\rho)\left[Y_L(\hat{\mathbf{r}})\otimes\boldsymbol{\nabla}\right]_J$$

Weak–nuclear interaction

$$\mathcal{T}_\sigma(\kappa, J_f) = \frac{4\pi G^2}{2J_i+1}\sum_{\mathsf{J}}\Big[|\langle J_f||\mathsf{O}_{\emptyset\mathsf{J}}||J_i\rangle|^2\mathcal{L}_\emptyset + \sum_{\mathsf{M}=0,\pm1}|\langle J_f||\mathsf{O}_{\mathsf{MJ}}||J_i\rangle|^2\mathcal{L}_{\mathsf{M}}$$
$$- 2\Re(|\langle J_f||\mathsf{O}_{\emptyset\mathsf{J}}||J_i\rangle\langle J_f||\mathsf{O}_{0\mathsf{J}}||J_i\rangle)\mathcal{L}_{\emptyset 0}\Big].$$

$L_;$ L_M $L_{;0}$ Lepton Traces

☺ For natural parity states with $\pi=(-)^J$,i.e., 0^+, 1^- , 2^+, 3^-….

$$\mathsf{O}_{\emptyset\mathsf{J}} = g_V\mathcal{M}^V_{\mathsf{J}}$$
$$\mathsf{O}^{CVC}_{0\mathsf{J}} = \frac{k_\emptyset}{\kappa}g_V\mathcal{M}^V_{\mathsf{J}}$$
$$\mathsf{O}_{0\mathsf{J}} = 2\overline{g}_V\mathcal{M}^V_{0\mathsf{J}} - \overline{g}_V\mathcal{M}^V_{\mathsf{J}}$$
$$\mathsf{O}_{\mathsf{M}\neq 0\mathsf{J}} = (\mathsf{M}g_A - \overline{g}_W)\hat{\mathcal{M}}^A_{1\mathsf{J}} + 2\overline{g}_V\tilde{\mathcal{M}}^V_{1\mathsf{J}}$$

☺ For unnatural parity states with $\pi=(-)^{J+1}$,i.e., 0^-, 1^+ ,2^-, 3^+….

$$-i\mathsf{O}_{\emptyset\mathsf{J}} = 2\overline{g}_A\mathcal{M}^A_{\mathsf{J}} + (\overline{g}_A + \overline{g}_{P1})\mathcal{M}^A_{0\mathsf{J}}$$
$$-i\mathsf{O}_{0\mathsf{J}} = (\overline{g}_{P2} - g_A)\mathcal{M}^A_{0\mathsf{J}}$$
$$-i\mathsf{O}_{\mathsf{M}\neq 0\mathsf{J}} = (-g_A + \mathsf{M}\overline{g}_W)\tilde{\mathcal{M}}^A_{1\mathsf{J}} + 2\mathsf{M}\overline{g}_V\hat{\mathcal{M}}^V_{1\mathsf{J}}$$

(i) deForest Jr.& Walecka, Adv.Phys15, 1(1966)
(ii) Kuramoto etal. NPA 512, 711 (1990)
(iii) Luyten etal. NP41,236 (1963)(μ-capture)
(iv) Krmpotic etal. PRC71, 044319(2005).

≈ all are equivalents.

$$\mathsf{O}_{\emptyset\mathsf{J}} = \hat{\mathcal{M}}_{\mathsf{J}},$$
$$\mathsf{O}_{\mathsf{MJ}} = \begin{cases} \hat{\mathcal{L}}_{\mathsf{J}}, & \text{for} \quad \mathsf{M}=0 \\ -\frac{1}{\sqrt{2}}\left[\mathsf{M}\hat{\mathcal{T}}^{MAG}_{\mathsf{J}} + \hat{\mathcal{T}}^{EL}_{\mathsf{J}}\right], & \text{for} \quad \mathsf{M}=\pm1 \end{cases}$$

Nuclear Structure Models

(i) Models with **microscopical formalism** with detailed nuclear structure, solves the microscopic quantum-mechanical Schrodinger or Dirac equation, provides nuclear wave functions and (g.s.-shape E_{sp} , J^{π} , log (ft), $\tau_{1/2}$ ...)

Examples:

Shell Model (Martinez et al. PRL83, 4502(1999))

RPA models

Self-Consistent Skyrme-HFB+QRPA

(Engel etal. PRC60, 014302(1999))

QRPA, Projected QRPA

(Krmpotic etal. PLB319(1993)393.)

Relativistic QRPA

(N. Paar et al., Phys. Rev. C 69, 054303 (2004))

Density Functional+Finite Fermi Syst.

(Borzov etal. PRC62, 035501 (2000))

(ii) Models describing **overall nucler properties** statistically where the parameters are adjusted to exp. data, no nuclear wave funct., polynomial or algebraic express.

Examples:

Fermi Gas Model,

Gross Theory of β-decay (GTBD)

Takahashi etal. PTP41,1470 (1969)

New exponential law for β^{+}.....

(Zhang etal. PRC73,014304(2006))

$\tau_{1/2}$ (Kar etal., astro-ph/06034517(2006))

Nuclear Structure Models

QRPA: Quasiparticle Random Phase Approximation

$$(e_t - \lambda_t)(u_t^2 - v_t^2) + u_t v_t \Delta_t = 0,$$

$$\begin{pmatrix} \mathcal{A} & \mathcal{B} \\ \mathcal{B} & \mathcal{A} \end{pmatrix} \begin{pmatrix} X \\ Y \end{pmatrix} = \omega \begin{pmatrix} X \\ -Y \end{pmatrix},$$

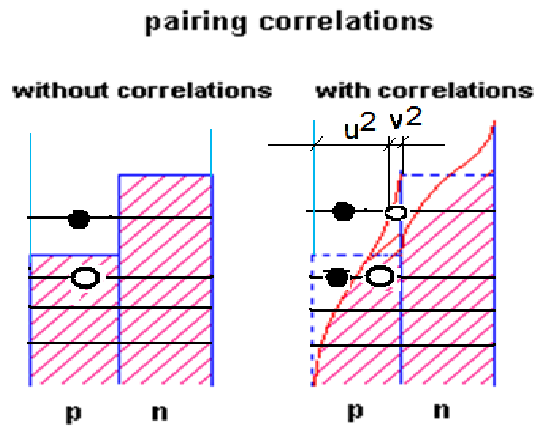

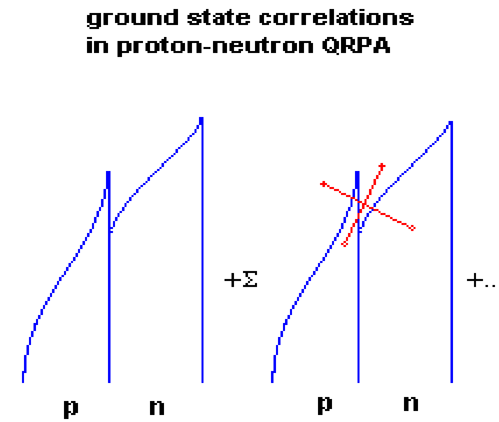

$$\langle BCS|\hat{N}|BCS\rangle \equiv \sum_{t=n(p)} (2j_t + 1) v_{j_t}^2 = N(Z),$$

PQRPA: Projected QRPA

$$2\hat{e}_p u_p v_p - \Delta_p (u_p^2 - v_p^2) \;=\; 0,$$

$$\begin{pmatrix} \mathcal{A}_\mu & \mathcal{B} \\ -\mathcal{B}^\dagger & -\mathcal{A}^*_{-\mu} \end{pmatrix} \begin{pmatrix} \mathcal{X}_\mu \\ \mathcal{Y}_\mu \end{pmatrix} = \Omega_\mu \begin{pmatrix} \mathcal{X}_\mu \\ \mathcal{Y}_\mu \end{pmatrix},$$

Particle number is conserved exactly .

Krmpotic etal. PLB319(1993)393.

$$V = -4\pi \, (v_s P_s + v_t P_t) \, \delta(r),$$

Nuclear Structure Models

RQRPA: Relativistic Quasiparticle Random Phase *

$$(e_t - \lambda_t)(u_t^2 - v_t^2) + u_t v_t \Delta_t = 0,$$

$$\begin{pmatrix} \mathcal{A} & \mathcal{B} \\ \mathcal{B} & \mathcal{A} \end{pmatrix} \begin{pmatrix} X \\ Y \end{pmatrix} = \omega \begin{pmatrix} X \\ -Y \end{pmatrix},$$

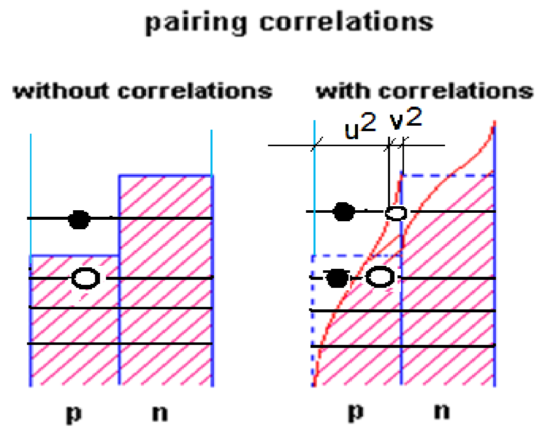

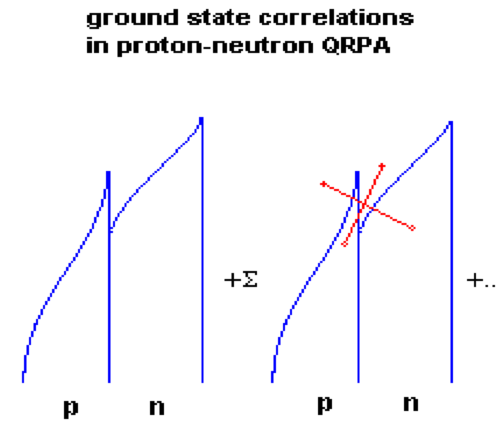

- RQRPA where both the mean field and the residual interaction are derived from the same effective Lagrangian density [9]. The ground state is calculated in the Relativistic Hartree-Bogoliubov (RHB) model using effective Lagrangians with density dependent meson-nucleon couplings and DD-ME2 parameterization, and pairing correlations are described by the finite range Gogny force. The HO basis with $N = 20$ or $N = 30$ is used only in the RHB calculation in order to determine the ground state and the single-particle spectra. The wave functions employed in RPA equations are obtained by converting the original basis to the coordinate representation, and the size of the RQRPA configuration space is limited by $2qp$ energy cut-offs E_{2qp}.

* N. Paar et al., Phys. Rev. C 69, 054303 (2004)

Weak Observable Constrains

QRPA/PQRPA in ^{12}C

Gamow -Teller Strengths of Beta decay

$$\widetilde{S}_\mu(J_f, E) = \frac{\eta}{\pi}\sum_f \frac{\widetilde{S}_\mu(J_f)}{\eta^2 + (E-\omega_{J_f})^2}, \qquad S_\mu(J_f) = \left|\langle J_f, Z+\mu, N-\mu || O_J || 0^+\rangle\right|^2.$$

$O_{J=0+}=1$, $O_{J=1+}=\sigma$

Volpe et al. PRC 62, 015501 (2000)``difficulties in choosing the g.s. of 12N because the lowest state is not the most collective one"

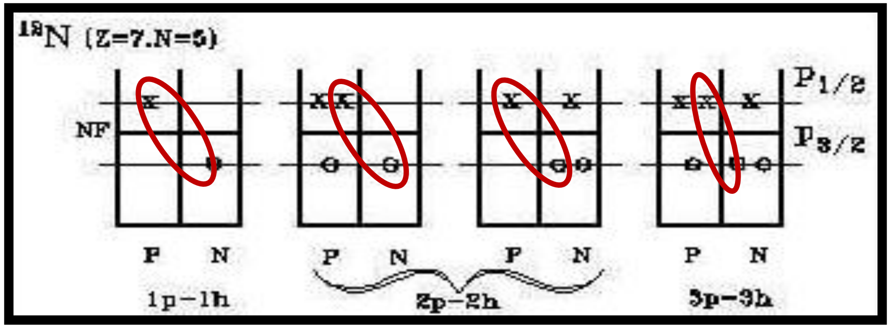

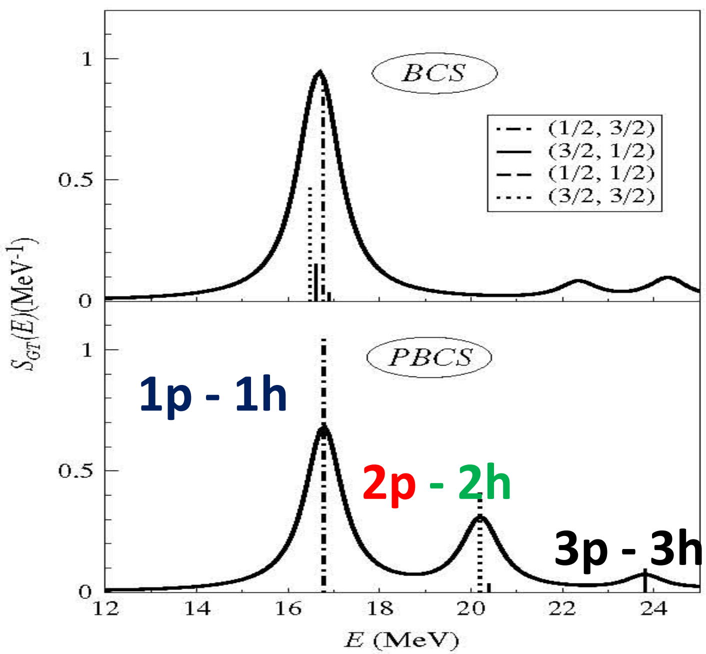

QRAP **Quasiparticle RAndom Phase code**

A. Samana, F. Krmpotic & C. Bertulani
Comp. Phys. Comm. 181 (2010)1123.

$$V = -4\pi\,(v_s P_s + v_t P_t)\,\delta(r),$$

PH-channel parameters from a systematic study GT resonances, F.K.&S.S. NPA 572, 329(1994)

P (I) : $v_s^{ph} = v^{pair}$, $v_t^{ph} = v_s^{ph}/0.6$

P(II): $v_s^{ph} = 27$, $v_t^{ph} = 64$

$$(v_s^{\rm pp} \equiv v_s^{\rm pair} \text{ and } v_t^{\rm pp} \gtrsim v_s^{\rm pp})$$

$$t = \frac{2v_t^{\rm pp}}{v_s^{\rm pair}(p) + v_s^{\rm pair}(n)},$$

Weak Observable Constrains

QRPA/PQRPA in ^{12}C

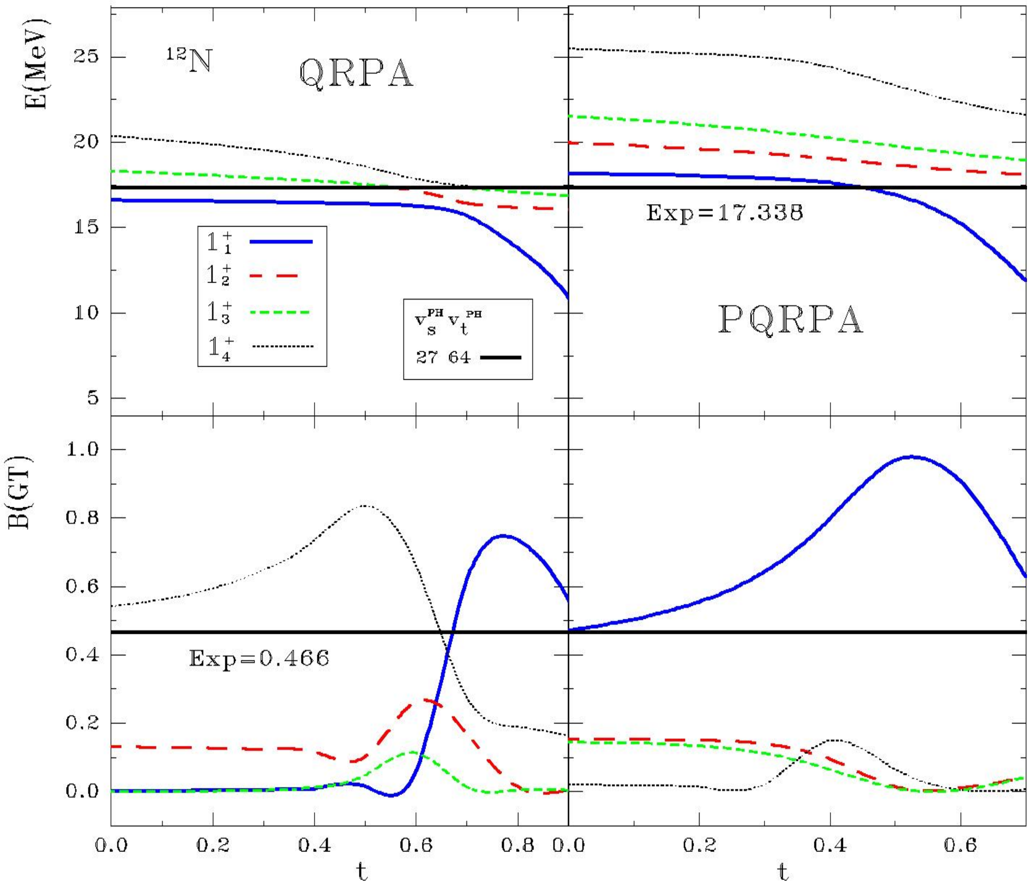

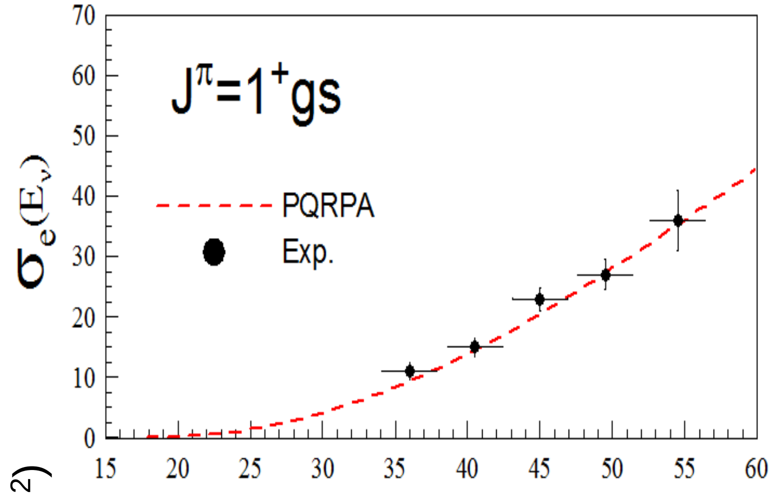

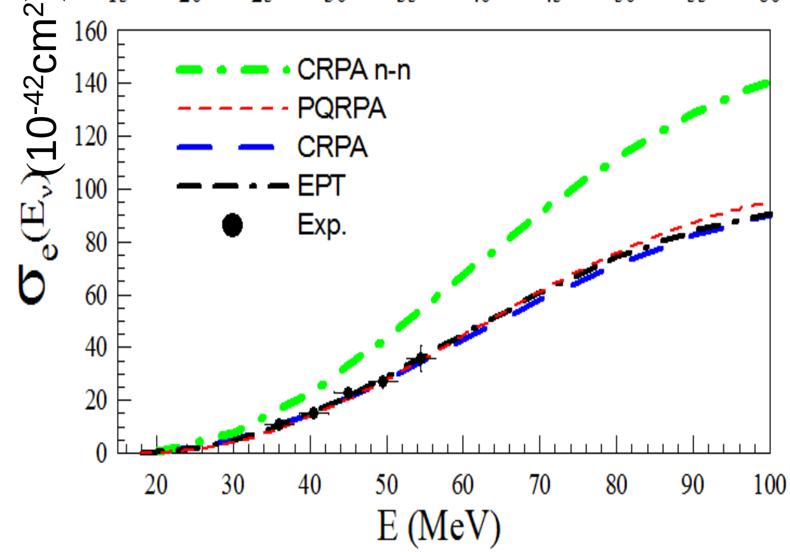

CRPA, Kolbe etal., PRC71, 044319(2005).
EPT, Mintz, PRC25,1671(1982).
PQRPA, Krmpotic etal., PRC71, 044319 (2005).
Exp, LSND coll., PRC55, 2078(1997).

Projection Procedure is Important!

Krmpotic etal. PRC71, 044319(2005).

Neutrino/antineutrino cross sections ^{12}C

QRPA/PQRPA in ^{12}C

SAMANA, KRMPOTIĆ, PAAR, AND BERTULANI PHYSICAL REVIEW C 83, 024303 (2011)

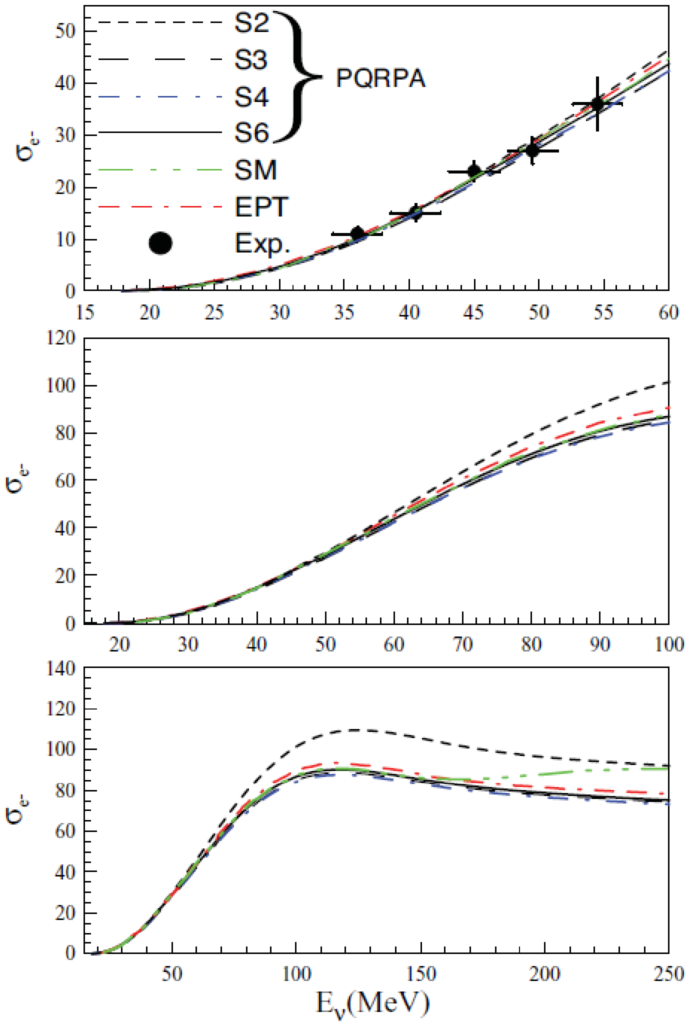

FIG. 3. (Color online) Same as Fig. 2, but here $t = 0$ for S_2 and S_3, $t = 0.2$ for S_4, and $t = 0.3$ for S_6. SM and EPT calculations are, respectively, from Refs. [98] and [16]. Experimental data in the DAR region are from Ref. [25].

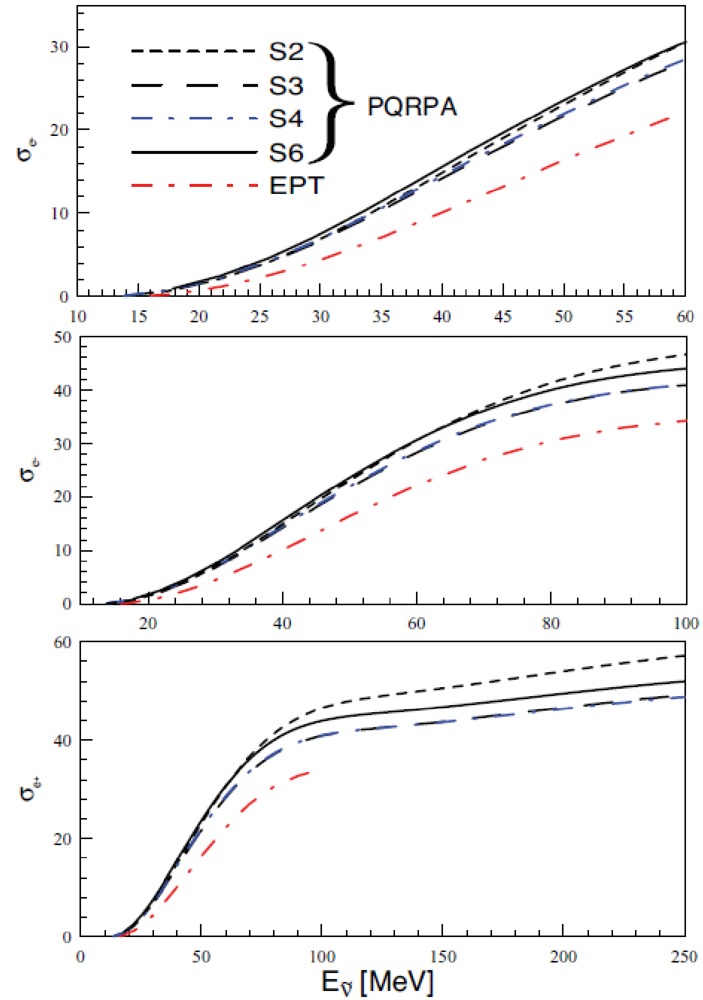

FIG. 4. (Color online) Calculated $^{12}C(\tilde{\nu}, e^+)^{12}B$ cross section $\sigma_{e^+}(E_{\tilde{\nu}}, 1_1^+)$ (in units of 10^{-42} cm^2), plotted as a function of the incident antineutrino energy $E_{\tilde{\nu}}$. As in Fig. 3, the value of t is 0 for s.p. spaces S_2, and S_3, 0.2 for S_4, and 0.3 for S_6. The EPT calculation from Ref. [16] is also shown.

Neutrino/antineutrino cross sections ^{12}C

QRPA/PQRPA in ^{12}C

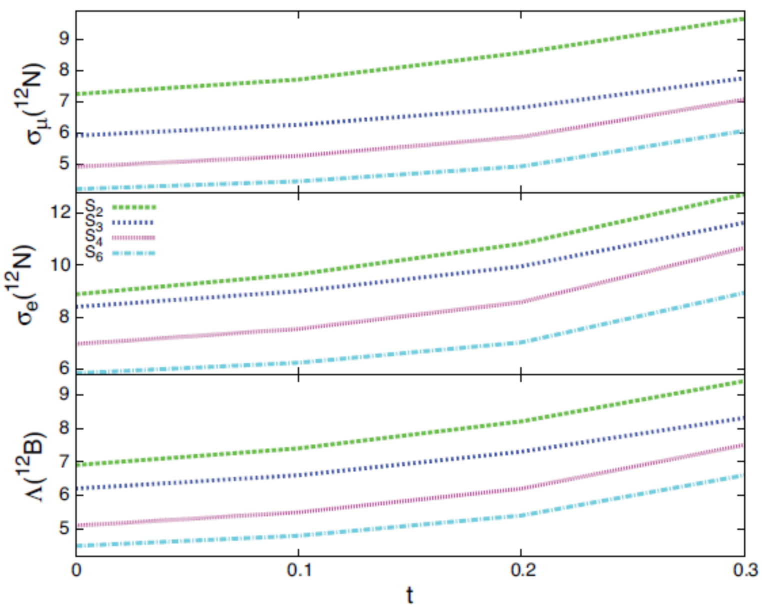

FIG. 5. (Color online) Muon-capture transition rate to the ^{12}B ground state (in units of 10^2 s^{-1}, and electron and muon folded ECSs to the ^{12}N ground state in units of 10^{-42} cm^2 and 10^{-41} cm^2, respectively. Experimental values, in these units, are $\Lambda(^{12}\mathrm{B}) = 6.2 \pm 0.3$ [45], $\overline{\sigma}_e(^{12}\mathrm{N}) = 9.1 \pm 0.4 \pm 0.9$ [25], and $\overline{\sigma}_e(^{12}\mathrm{N}) = 8.9 \pm 0.3 \pm 0.9$ [26] and $\overline{\sigma}_\mu(^{12}\mathrm{N}) = 6.6 \pm 1.0 \pm 1.0$ [28], and $\overline{\sigma}_\mu(^{12}\mathrm{N}) = 5.6 \pm 0.8 \pm 1.0$ [29], respectively.

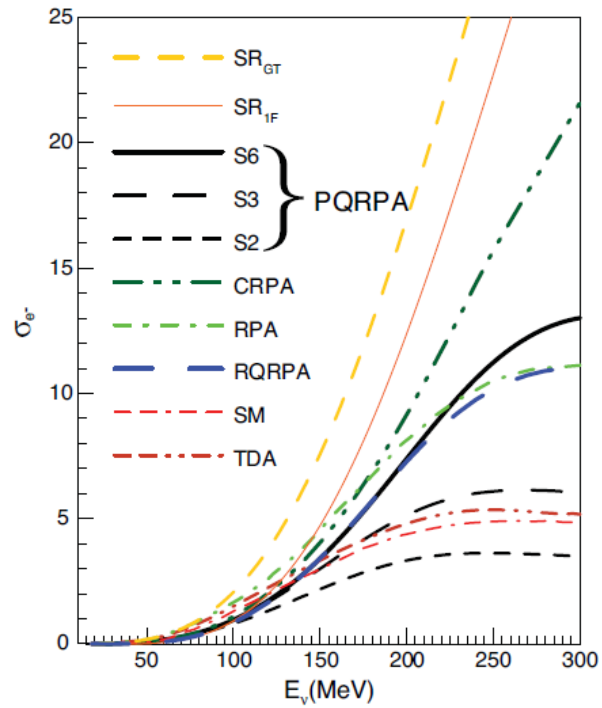

FIG. 6. (Color online) Inclusive $^{12}\mathrm{C}(\nu, e^-)^{12}\mathrm{N}$ cross section $\sigma_{e^-}(E_\nu)$ (in units of 10^{-39} cm^2) plotted as a function of the incident neutrino energy E_ν. PQRPA results within s.p. spaces S_2, S_3, and S_6, and with the same values of $s = t$ as in Fig. 3, are compared with two sum-rule limits (as explained in the text), $\mathrm{SR_{GT}}$ and $\mathrm{SR_{1F}}$, obtained with an average excitation energy $\overline{\omega_{J_n^\pi}}$ of 17.34 and 42 MeV, respectively. Several previous RPA-like calculations, namely, the RPA [43], CRPA [102], and RQRPA within S_{20} for $E_{2qp} = 100$ MeV [51], as well as the SM [43] and the TDA [34], are also shown.

Neutrino/antineutrino cross sections ^{12}C

QRPA/PQRPA in ^{12}C

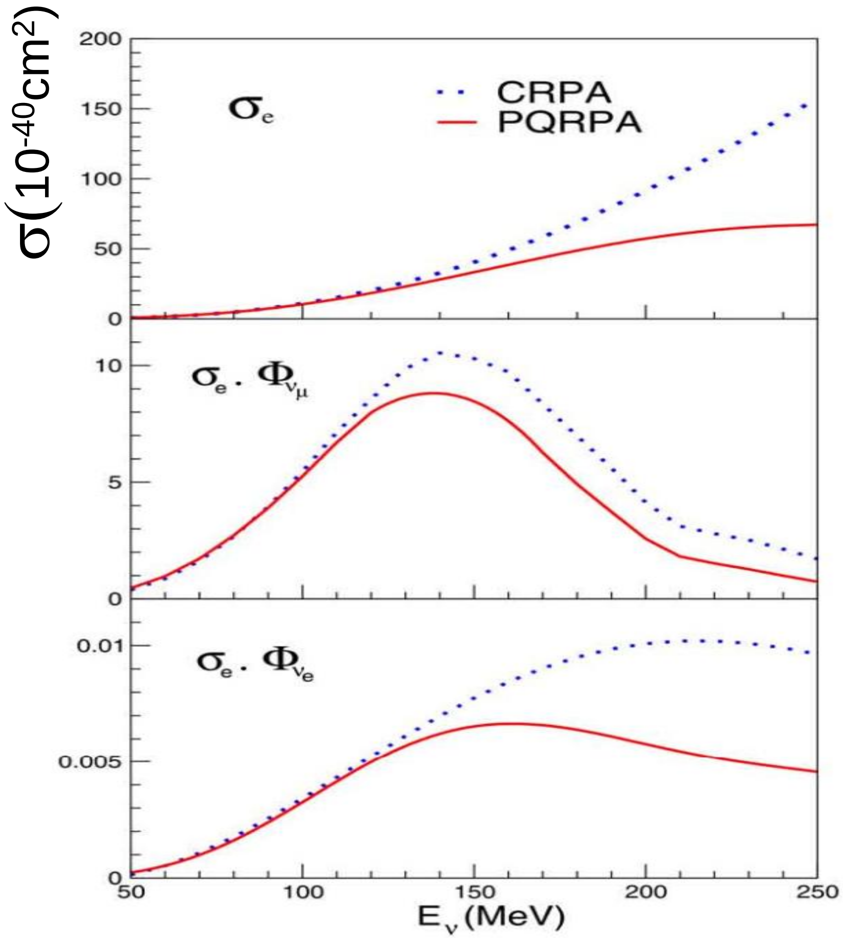

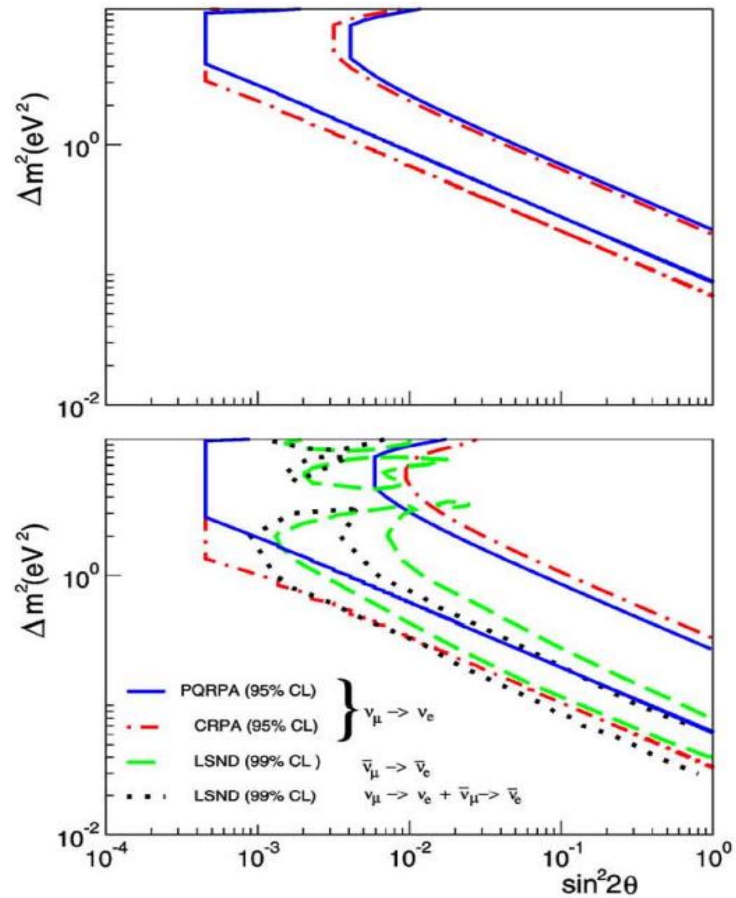

ν-nucleus cross section are important to constrain parameters in neutrino oscillations.

$$\overline{\nu}_{\mu} \rightarrow \overline{\nu}_{e} \qquad \nu_{\mu} \rightarrow \nu_{e}$$

* Increase probability oscillations.

* Confidence level region is diminished by difference in σ_e between PQRPA and CRPA,

A.Samana,et al.,PLB (2005) 100

Neutrino/antineutrino cross sections ^{12}C

QRPA/PQRPA/RQRPA in ^{12}C

SAMANA, KRMPOTIĆ, PAAR, AND BERTULANI PHYSICAL REVIEW C **83**, 024303 (2011)

TABLE I. Fraction (in %) of flux-averaged cross sections $\overline{\sigma}_{e^+}$ for $^{12}C(\tilde{\nu}, e^+)^{12}B$ for allowed (A), first forbidden (1F), second forbidden (2F), and third forbidden (3F) processes. Antineutrino fluxes $n_{e^+}(E_{\tilde{\nu}})$ are the same as in Ref. [108], that is, the DAR flux, and those produced by boosted ^{6}He ions with different values of $\gamma = 1/\sqrt{1 - v^2/c^2}$. Results of two calculations are presented: (i) PQRPA within S_5 and (ii) RQRPA within $N = 30$, with a cutoff $E_{2qp} = 300$ MeV.

	DAR	γ		
		6	10	14
A				
PQRPA	79.43	92.09	77.00	63.01
RQRPA	84.40	94.88	82.25	67.15
1F				
PQRPA	20.03	7.83	22.16	33.76
RQRPA	15.10	4.13	16.86	29.61
2F				
PQRPA	0.51	0.07	0.78	2.89
RQRPA	0.55	0.08	0.81	2.91
3F				
PQRPA	0.018	0.002	0.04	0.33
RQRPA	0.025	0.011	0.05	0.33

$$n_e(E_\nu) = \frac{0.5546}{T_\nu^3} \frac{E_\nu^2}{e^{E_\nu/T_\nu} + 1}$$

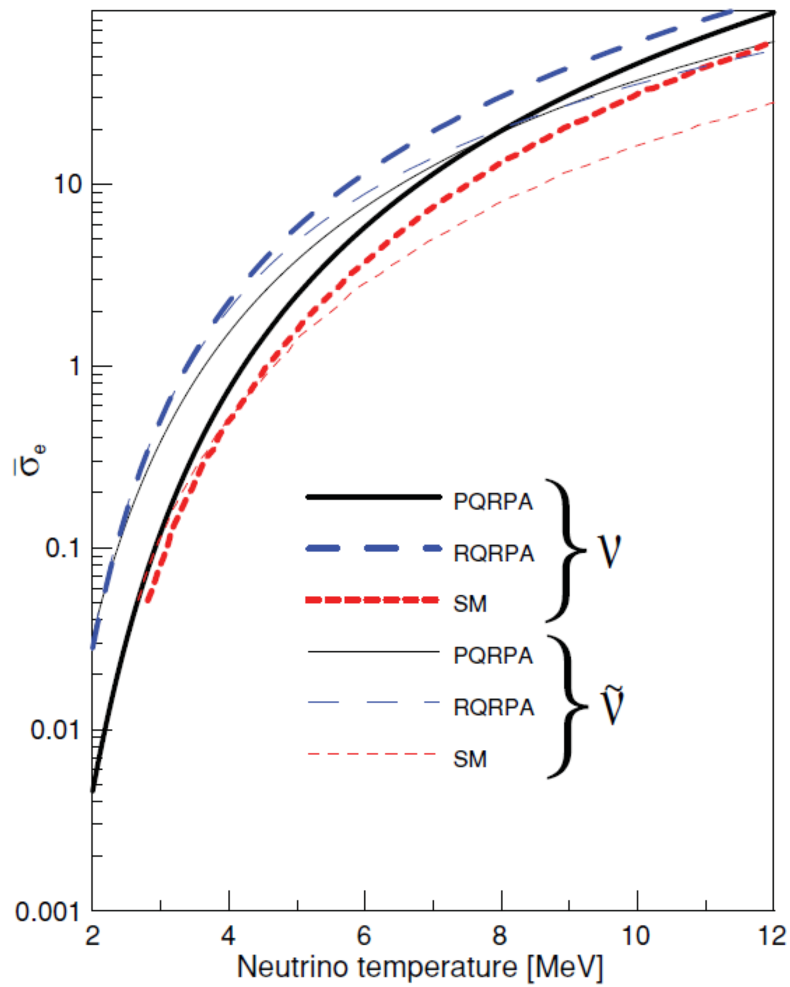

FIG. 13. (Color online) Flux-averaged neutrino and antineutrino cross sections $\overline{\sigma}_{e^\pm}$ in ^{12}C with typical supernova fluxes.

Neutrino/antineutrino cross sections ^{56}Fe

QRPA/PQRPA in ^{56}Fe

♣12 s.p. levels: 2, 3 and 4 $\hbar\varpi$,
♣ 3$\hbar\varpi$, s.p.e of ^{56}Ni, 2&4 s.p.e. H.O.

♣ v^{pair}_s (p,n) to Δ(p,n) experimental.
♣v^{ph}_s =24, v^{ph}_t =64,(MeV.fm^3) GT resonance in ^{48}Ca [NPA572,329(1994)].and t =0,

B(GT-) =17.7 ~ B(GT-)=18.68
Skyrme [NPA716,230(2003)] overestimates exp.
9.9±2.4 [NPA410,371(1983)].

$$\langle\sigma_e\rangle = \int dE_\nu \sigma(E_\nu) n(E_\nu),$$

$$n(E_\nu) = \frac{96E_\nu^2}{M_\mu^4}(M_\mu - 2E_\nu),$$

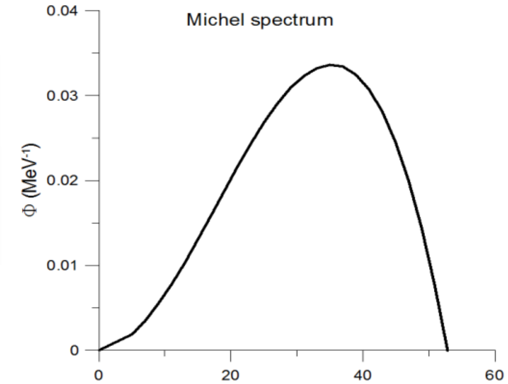

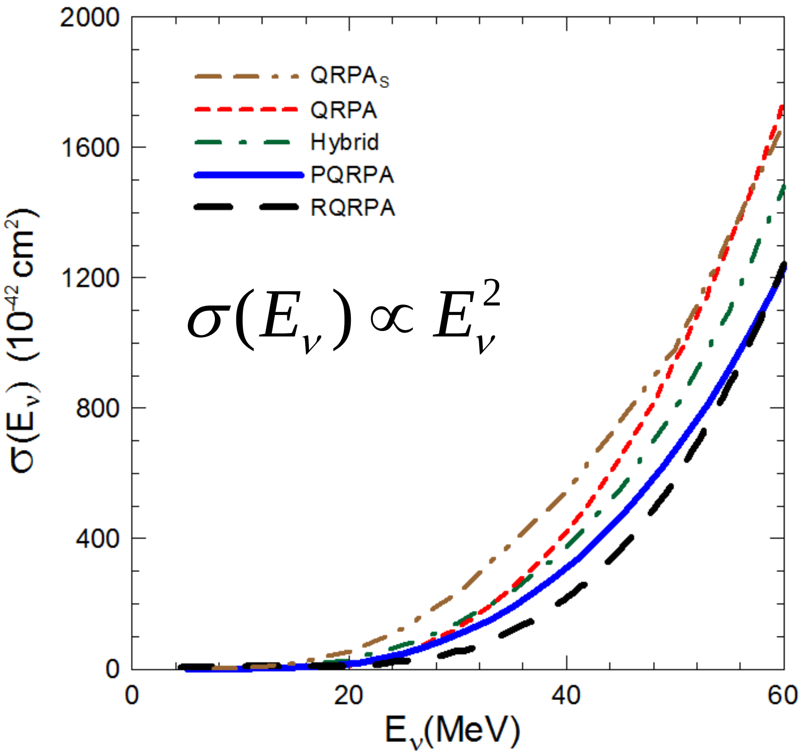

Model	$\langle\sigma_e\rangle$
QRPA	264.6
PQRPA	197.3
Hybrid$^{(a)}$ [14]	228.9
Hybrid$^{(b)}$ [14]	238.1
TM [26]	214
RPA [27]	277
QRPA$_S$ [15]	352
RQRPA [16]	140
Exp[5] **KARMEN**	$256 \pm 108 \pm 43$

A.Samana & C.Bertulani, PRC78, 024312 (2008)

Neutrino/antineutrino cross sections ^{56}Fe

QRPA/PQRPA – Beta decay strengths and Inclusive muon capture rates

- ♣12 s.p. levels: 2, 3 and 4 ħϖ,
- ♣3ħϖ, s.p.e of ^{56}Ni, 2&4 s.p.e. H.O.

$$\text{(i)}\ \text{QRPA1 e PQRPA1: } v_s^{ph} = 27 \text{ e } v_t^{ph} = 64 \text{ (MeV fm}^3\text{)},$$

$$\text{(ii)}\ \text{QRPA2 e PQRPA2: } v_s^{ph} = 55 \text{ e } v_t^{ph} = 92 \text{ (MeV fm}^3\text{)}.$$

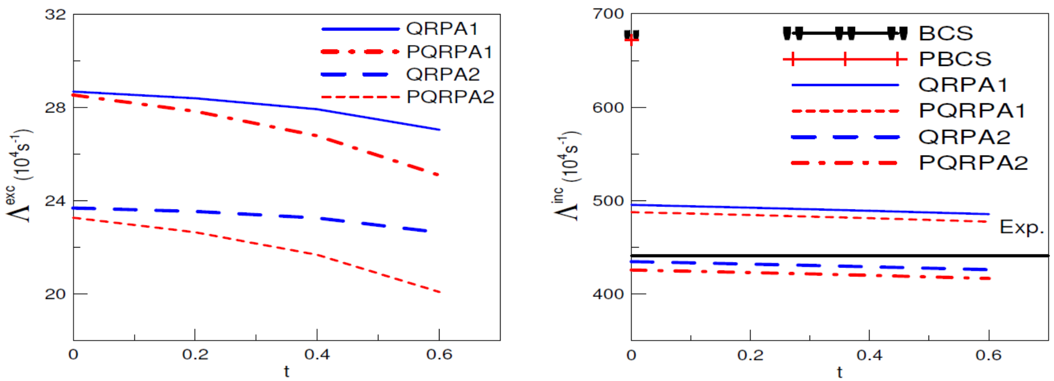

Figura 3.1: ^{56}Fe$(\mu^-, \nu_\mu)^{56}$Mn (em unidades de 10^4 s^{-1}); Painel esquerdo: Reações exclusivas, painel direito: Reações inclusivas. As taxas de captura calculadas no BCS, PBCS, QRPA e PQRPA são comparadas. Dados experimentais da Ref. [5] são também apresentados.

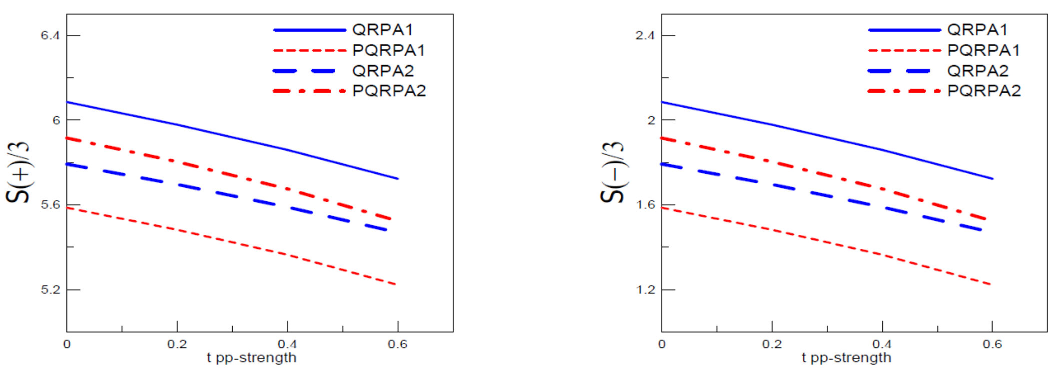

Figura 3.3: Amplitudes de Gamow-Teller $S(+)$ ^{56}Fe$(\nu, e^-)^{56}$Mn e $S(-)$ ^{56}Fe$(\nu, e^+)^{56}$Co.

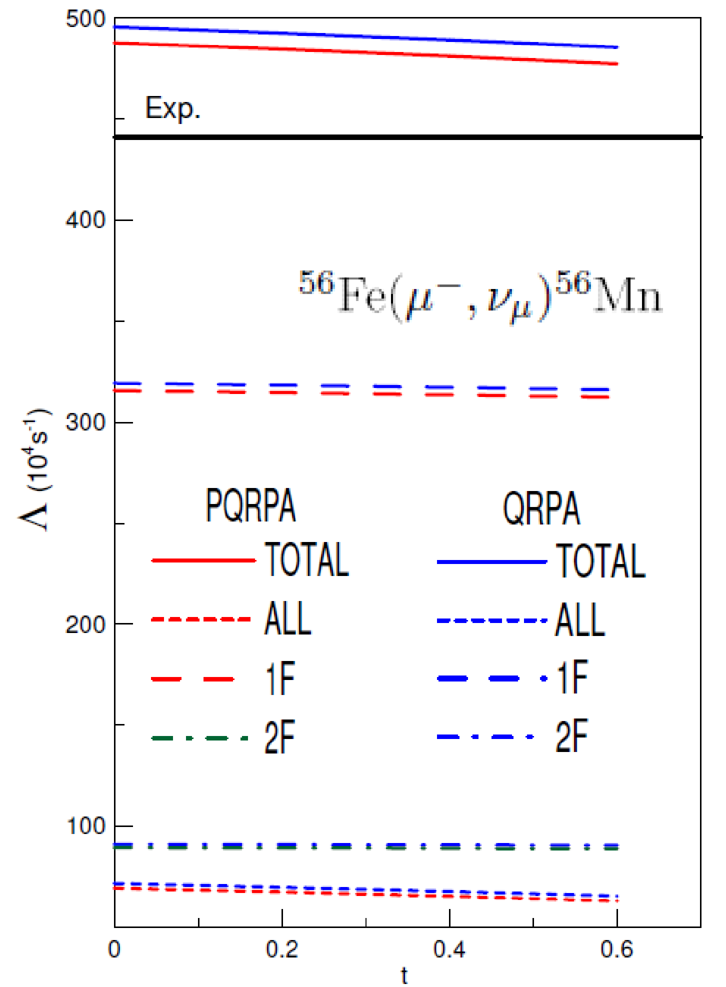

Neutrino/antineutrino cross sections ^{56}Fe

QRPA/PQRPA in ^{56}Fe

Supernovae Neutrinos – To estimate events in supernova detectors.

$$N_e \equiv N_e(T_{\nu_e}) = N_t \int_0^\infty F_e^0(E_\nu, T_{\nu_e})\sigma(E_\nu)\varepsilon(E_\nu)dE_\nu,$$

$$\tilde{N}_e \equiv \tilde{N}_e(T_{\nu_x}) = N_t \int_0^\infty F_x^0(E_\nu, T_{\nu_x})\sigma(E_\nu)\varepsilon(E_\nu)dE_\nu.$$

Effective temperature

Neutrino energy

Time-integrated energy

$$F_\alpha^0(E, T_\alpha, \eta_\alpha = 0, L_\alpha, D) = \frac{L_\alpha}{4\pi D^2 T_\alpha^4 F_3(0)} \frac{E^2}{e^{E/T_\alpha} + 1},$$

Distance to supernova

Norm.factor

Pinching parameter

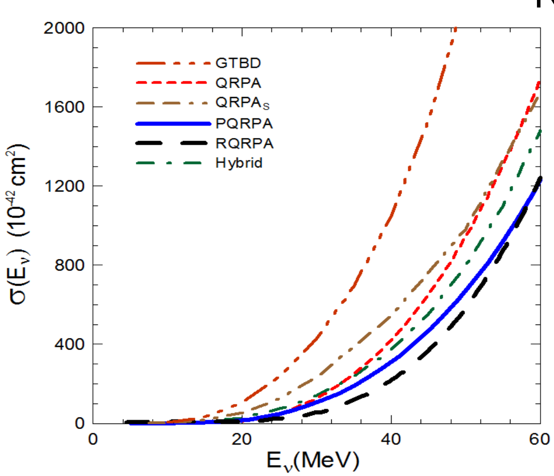

D~ 10 kpc,
$L_\alpha = E_b$. 1/6,
$E_b = 3\text{x}10^{53}$ erg,
$\alpha = \nu_\alpha = \{\nu_e, \nu_\mu, \nu_\tau\}$
$T(\nu_x)/T(\bar{\nu}_e) = 1.5$,
$T(\nu_e)/T(\bar{\nu}_e) = 0.8$,
$T(\bar{\nu}_e) = 5$ MeV

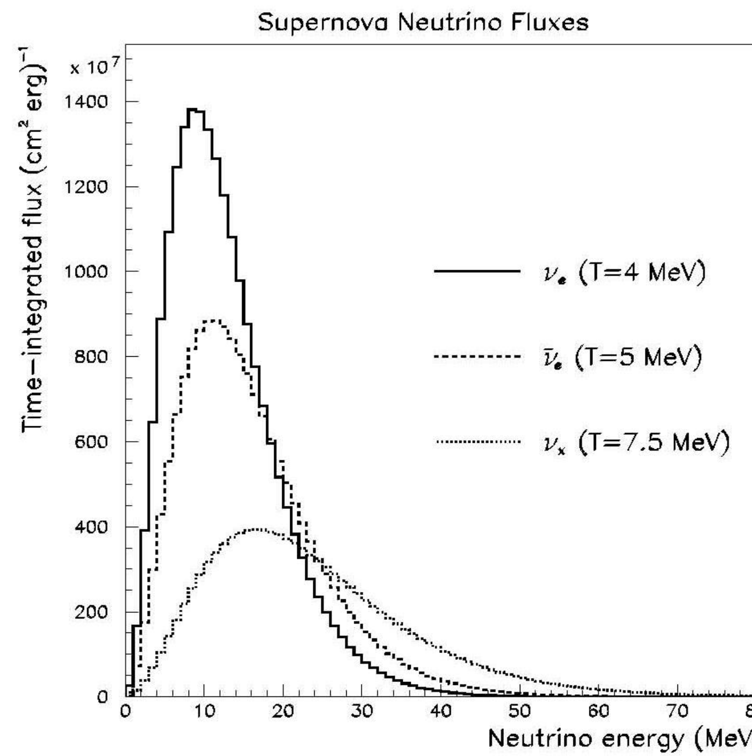

Fig. 1. Neutrino energy spectra at the neutrino-sphere.

Neutrino/antineutrino cross sections ^{56}Fe

$$\nu_e + {}^{56}Fe \rightarrow {}^{56}Co^* + e^-$$

A.S.& C.B., PRC 78, 024312 (2008)

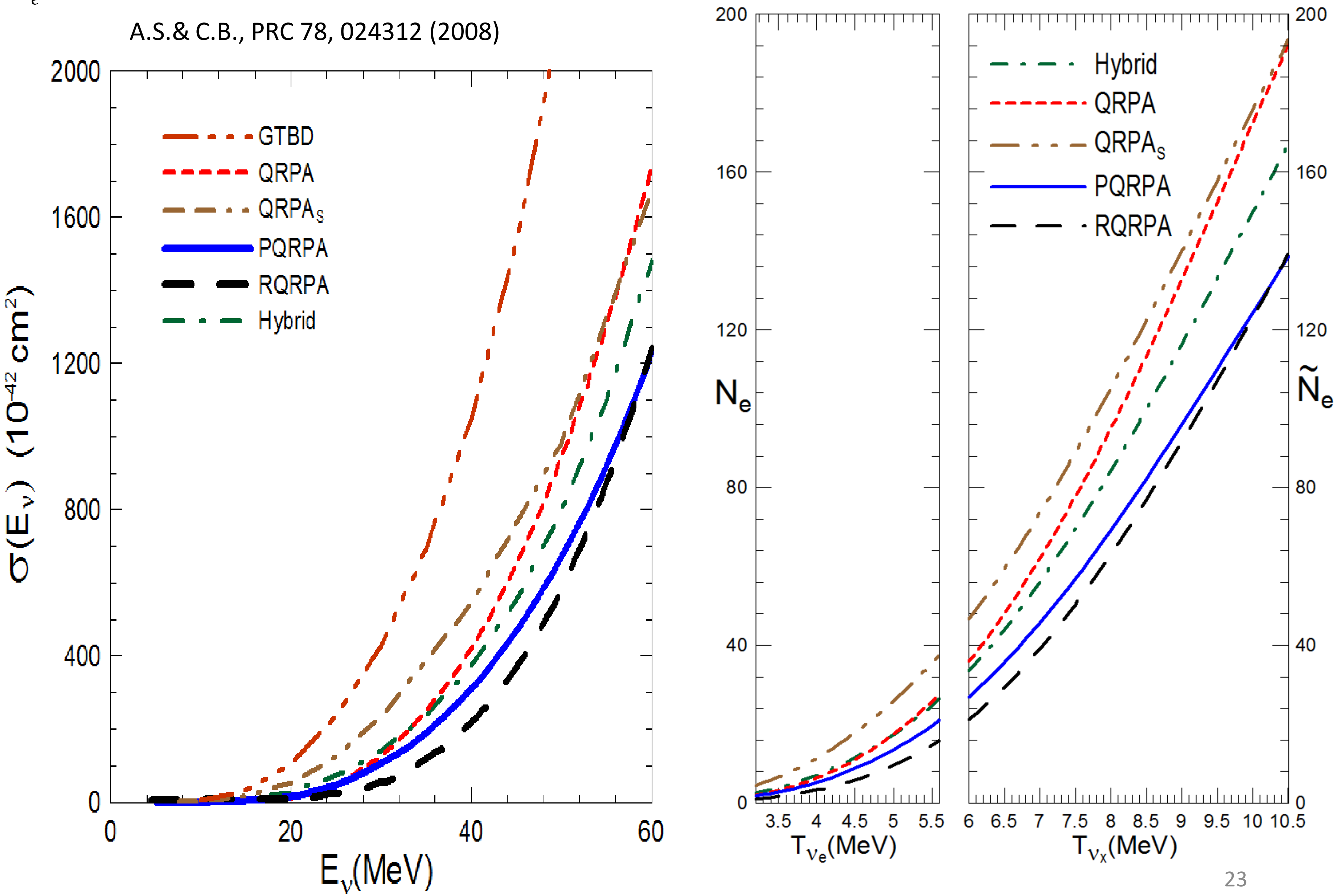

Neutrino/antineutrino cross sections ^{56}Fe

QRPA/PQRPA in ^{56}Fe

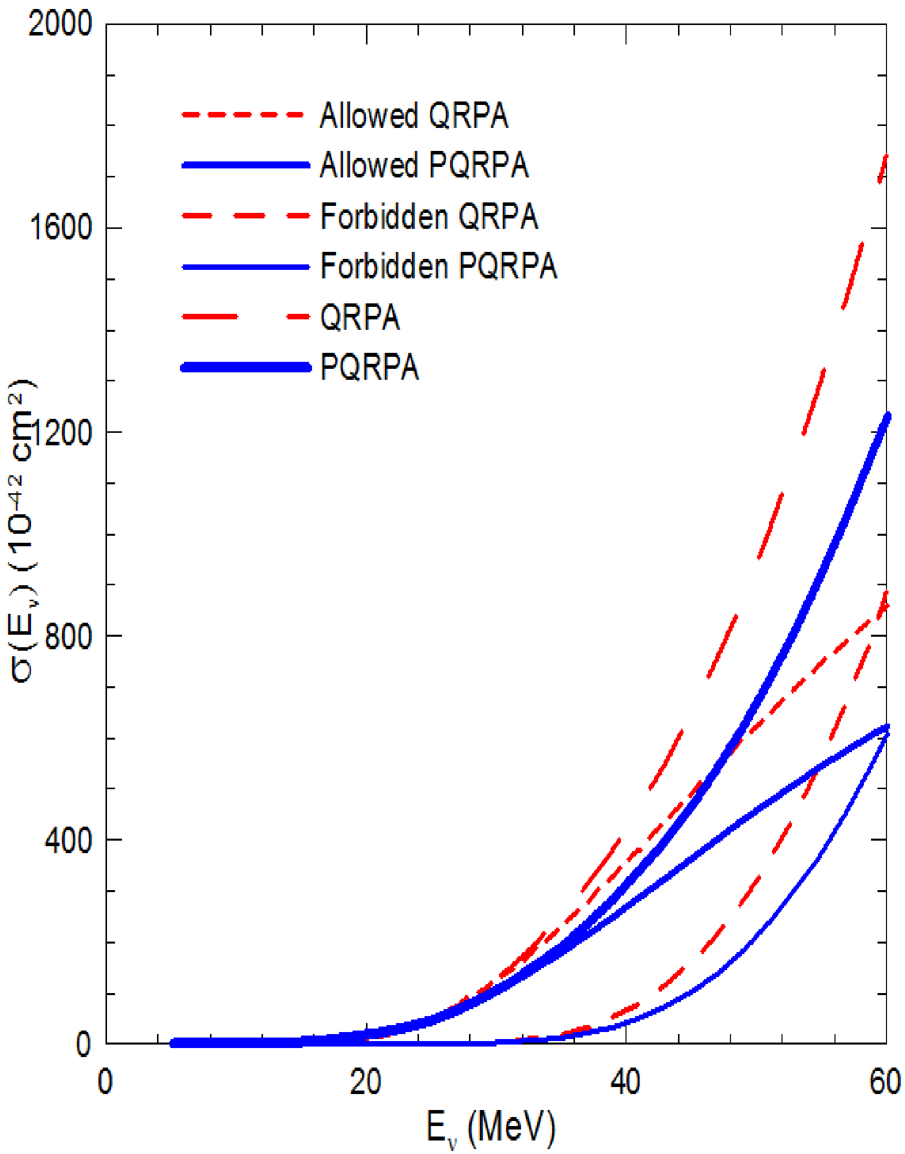

PQRPA & QRPA, PRC 78, 024312 (2008)

RQRPA DD-ME2 , PRC 77,024608 (2008)

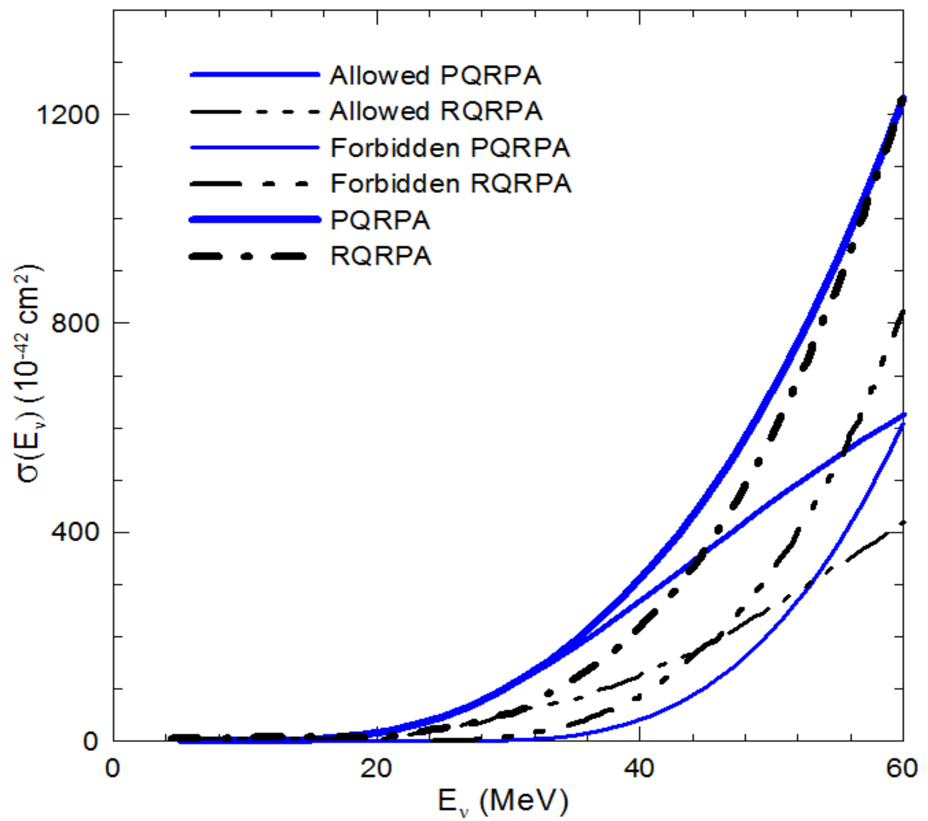

Neutrino/antineutrino cross sections ^{40}Ar

QRPA/PQRPA in ^{40}Ar – Weak observables constrains

- Gamow -Teller Strengths of Beta decay : low energy – GT resonances & IAS

- Inclusive – exclusive muon capture rates: high energy - 100 MeV muon mass

$$V = -4\pi \left(v_s P_s + v_t P_t \right) \delta(r),$$

PH-channel parameters from a systematic study GT resonances, F.Krmpotic & S. Sharma NPA 572, 329 (1994)

$v_s^{ph} = 27$, $v_t^{ph} = 64$

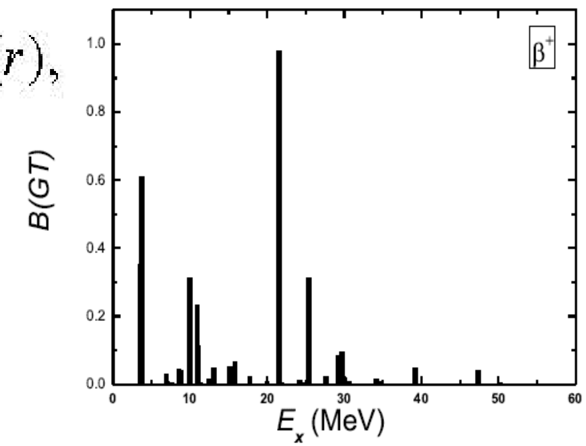

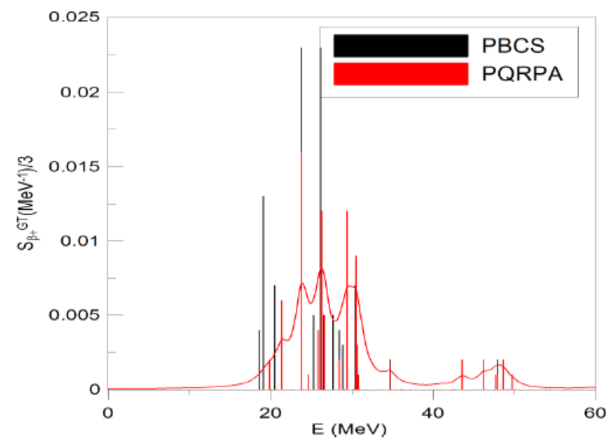

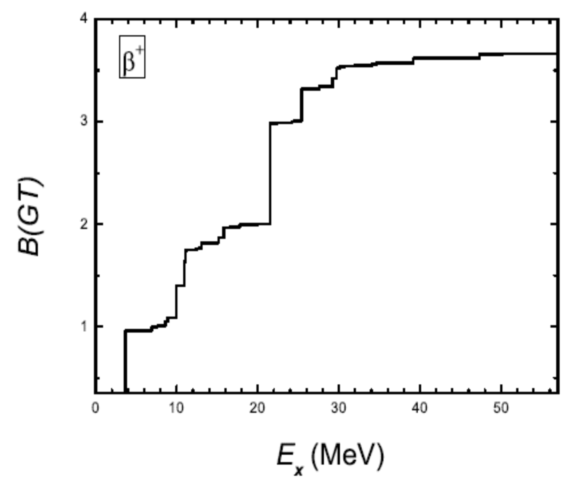

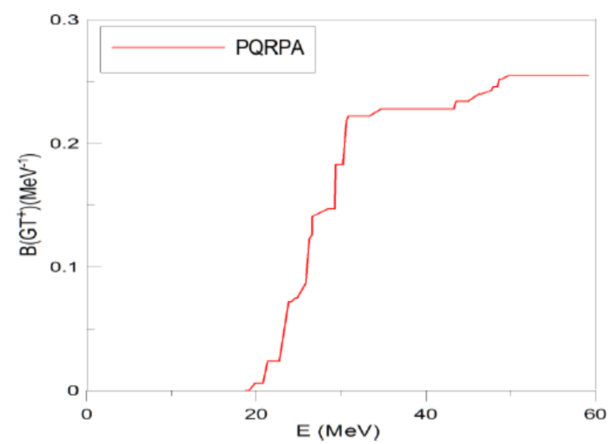

Neutrino/antineutrino cross sections ^{40}Ar

QRPA/PQRPA

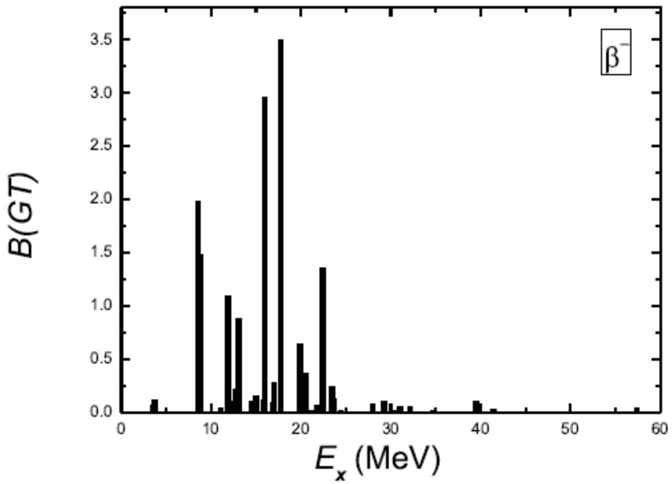

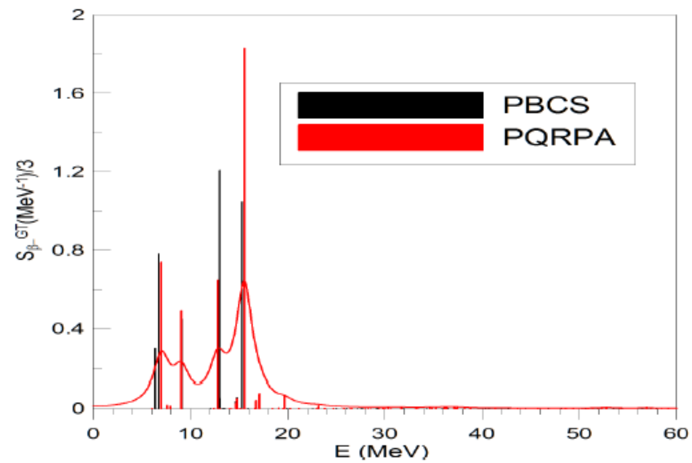

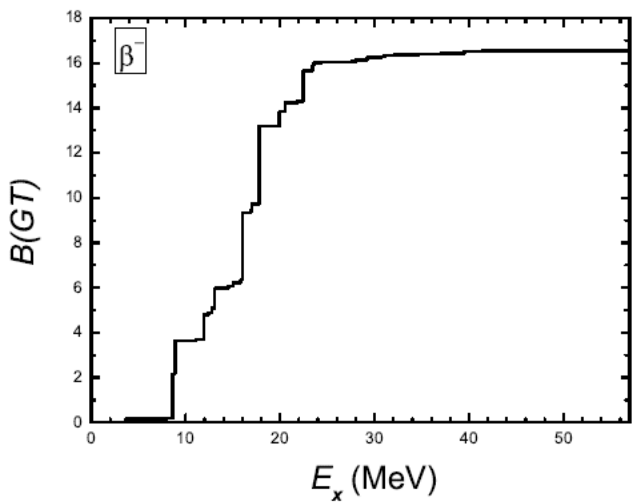

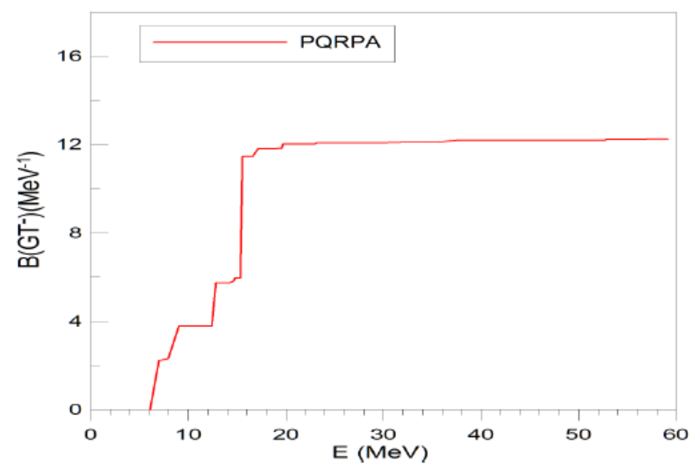

Neutrino/antineutrino cross sections ^{40}Ar

PQRPA/RQRPA systematic calculations

Muon capture rates within the projected QRPA
Danilo Sande Santos, Arturo R. Samana, Francisco Krmpotic, Alejandro J. Dimarco
http://pos.sissa.it/archive/conferences/142/120/XXXIV%20BWNP_120.pdf
Ratios of theoretical to experimental inclusive muon capture rates for different nuclear models, as function of the mass number *A*. The present QRPA and PQRPA results, as well as the RQRPA calculation [13] were done with *g*A = 1.135, while in the RPA+BCS model [11] was used the unquenched value *g*A = 1.26 for all multipole operators, except for the GT ones where it was reduced to *g*A ∼ 1.

(^{12}C, ^{20}Ne, ^{24}Mg, ^{28}Si, ^{40}Ar, ^{52}Cr, ^{54}Cr, ^{56}Fe)

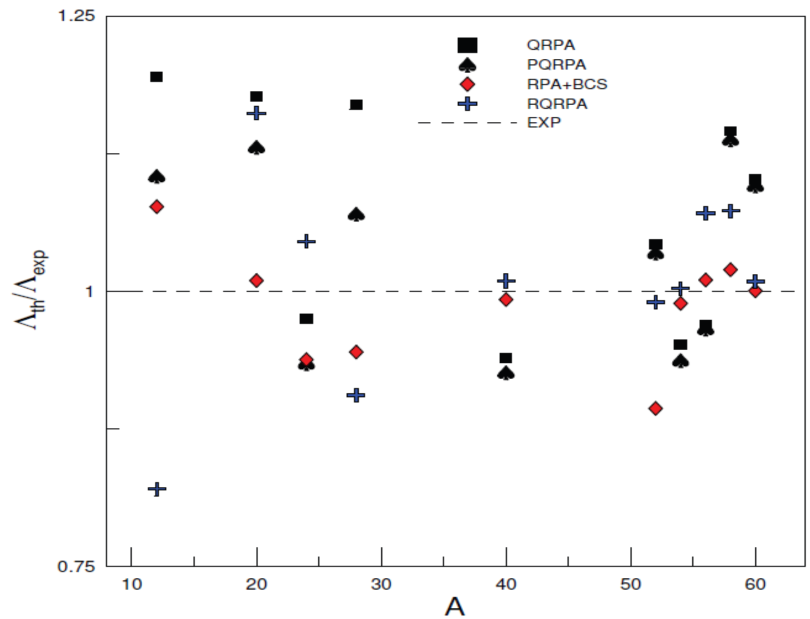

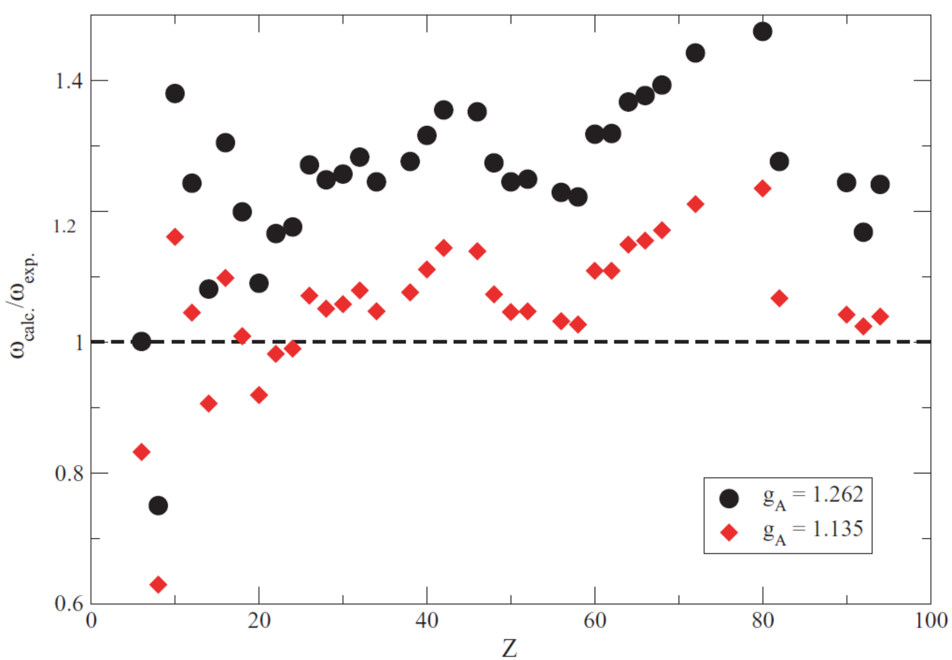

Relativistic quasiparticle random-phase approximation calculation of total muon capture rates, T. Marketin, N. Paar, T. Nikˇsi´c, and D. Vretenar, PHYSICAL REVIEW C **79**, 054323 (2009)
Ratio of the calculated and experimental total muon capture rates, as function of the proton number *Z*. Circles correspond to rates calculated with the free-nucleon weak form factors Eqs. (10)–(13) [21], and diamonds denote values obtained by quenching the free nucleon axial-vector coupling constant *gA* =1.262 to *gA* = 1.135 for all operators, i.e., in all multipole channels.

Neutrino/antineutrino cross sections ^{40}Ar

PQRPA - Inclusive muon capture rates

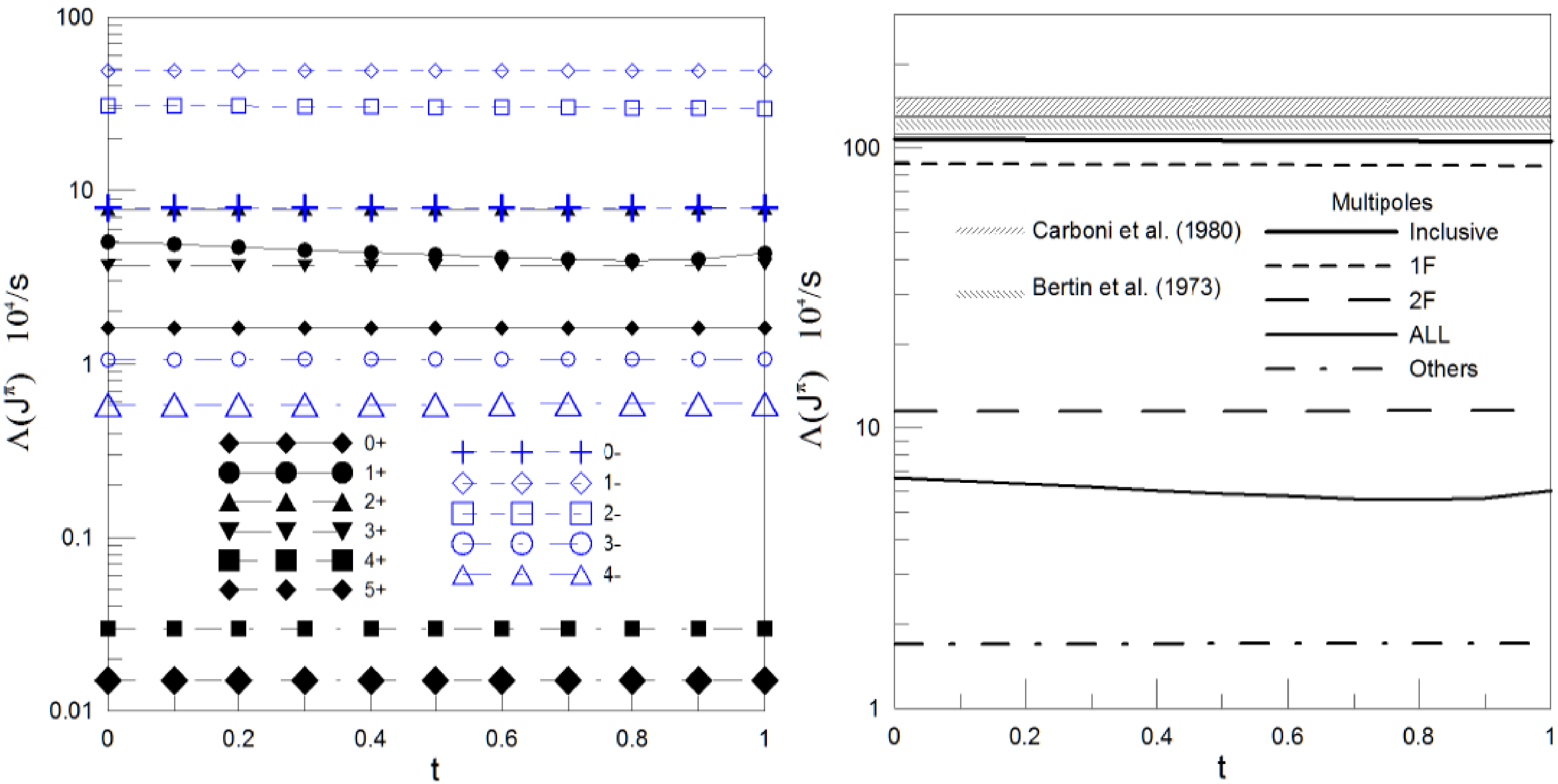

FIG. 3: Left Panel: Muon capture rates for different multipoles as function of the t pp-parameter of residual interaction. Right panel: Inclusive, allowed (ALL: $0^+, 1^+$), first forbidden (1F: $0^-, 1^-, 2^-$), second forbidden (2F: $2^+, 3^+$) and multipoles of superior order (up to $7^{\pm}$), muon capture rates for ^{40}Ar as a function of the t.

Neutrino/antineutrino cross sections ^{40}Ar

QRPA Cheoun et al. PRC83, 028801 (2011)/ PQRPA

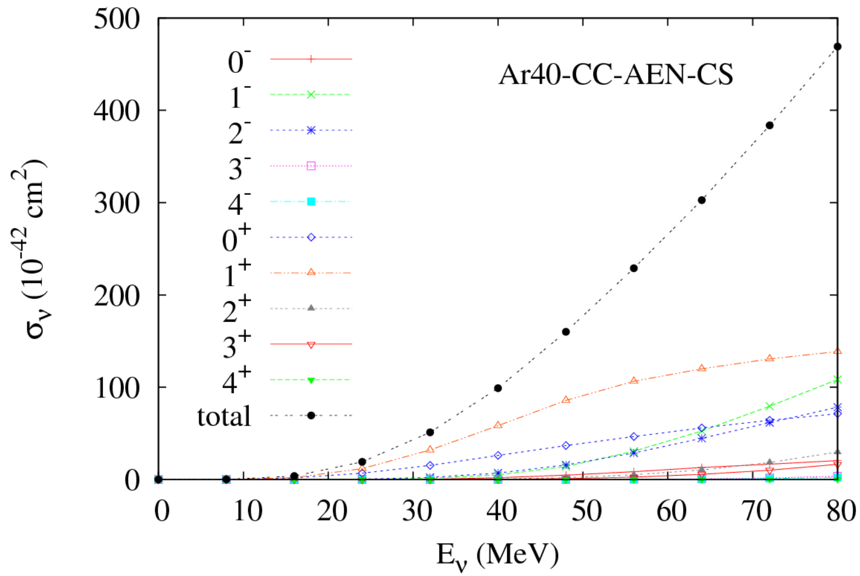

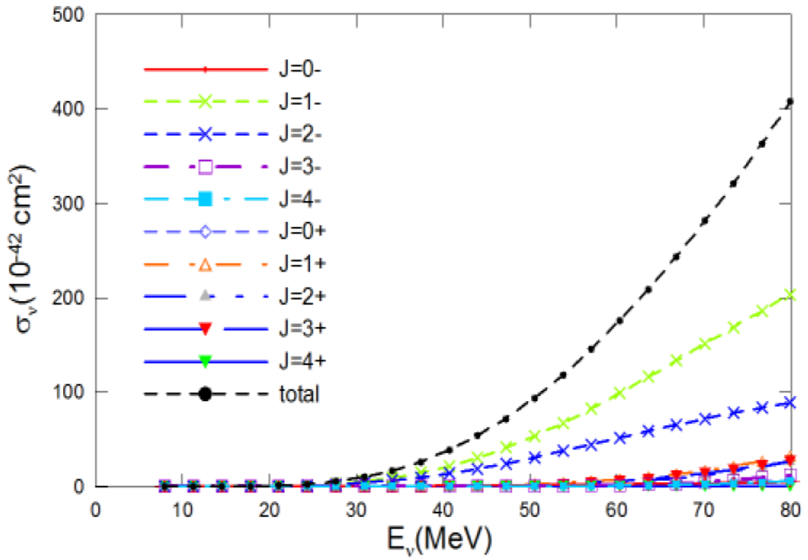

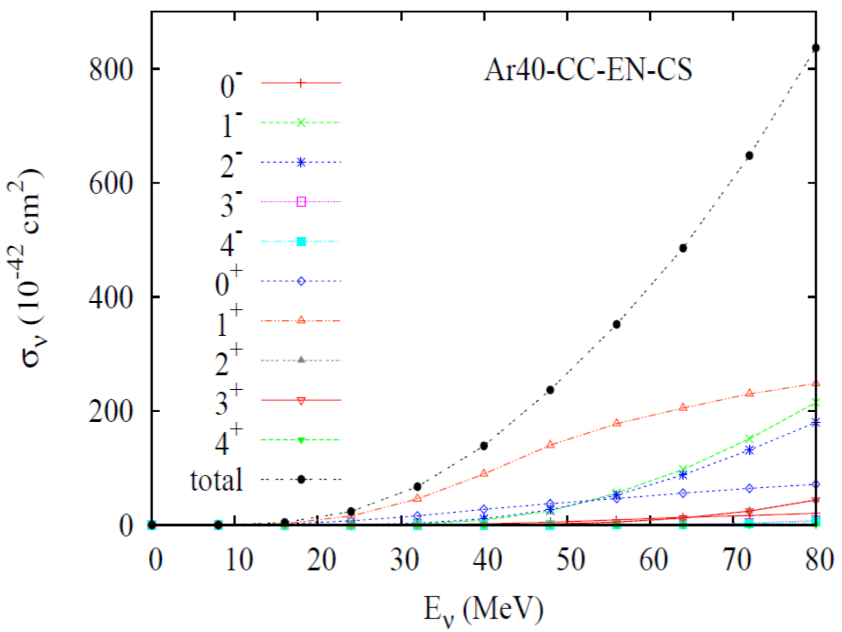

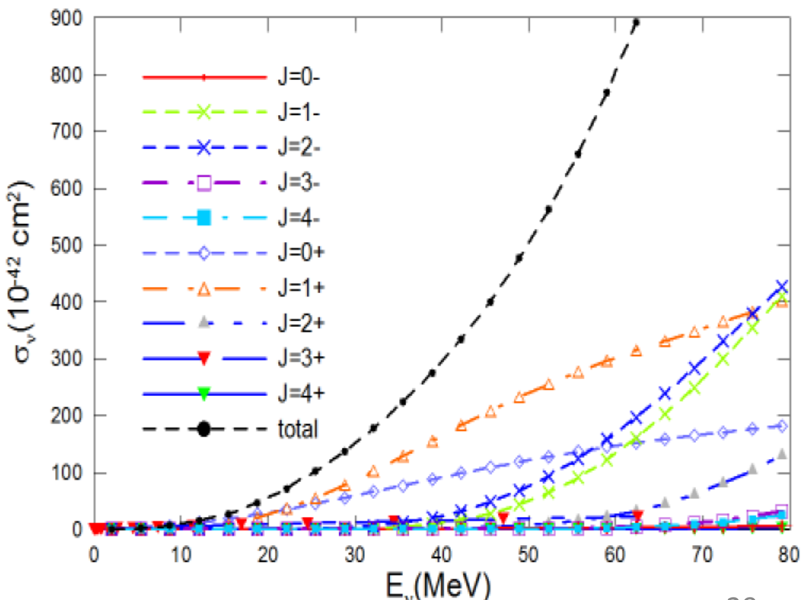

Supernovae Neutrinos – Signal Detection

SM + RPA (Suzuki & Honma)

PRC87, 014607(2013)

PQRPA

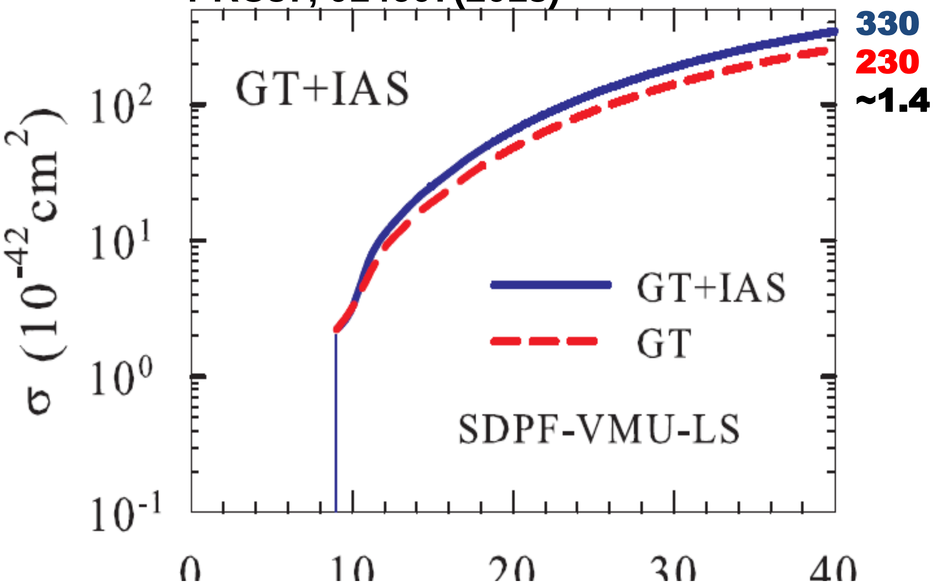

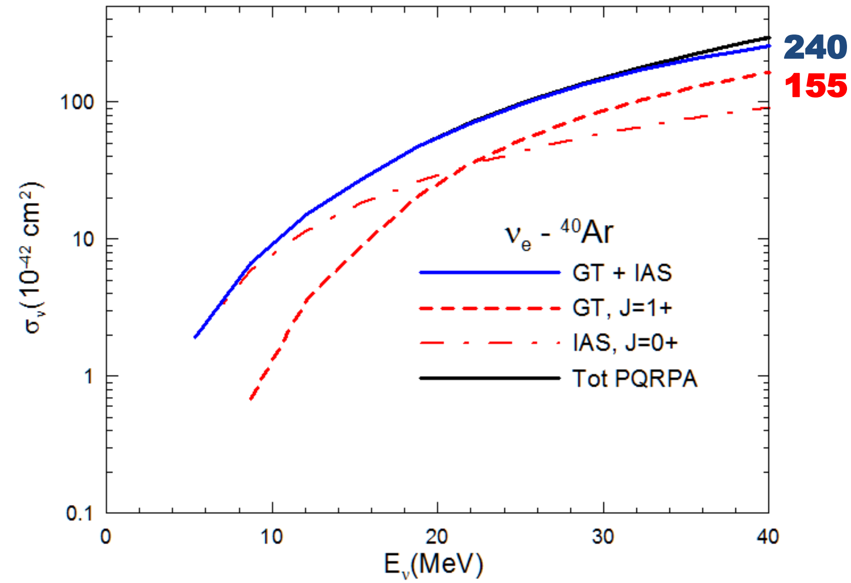

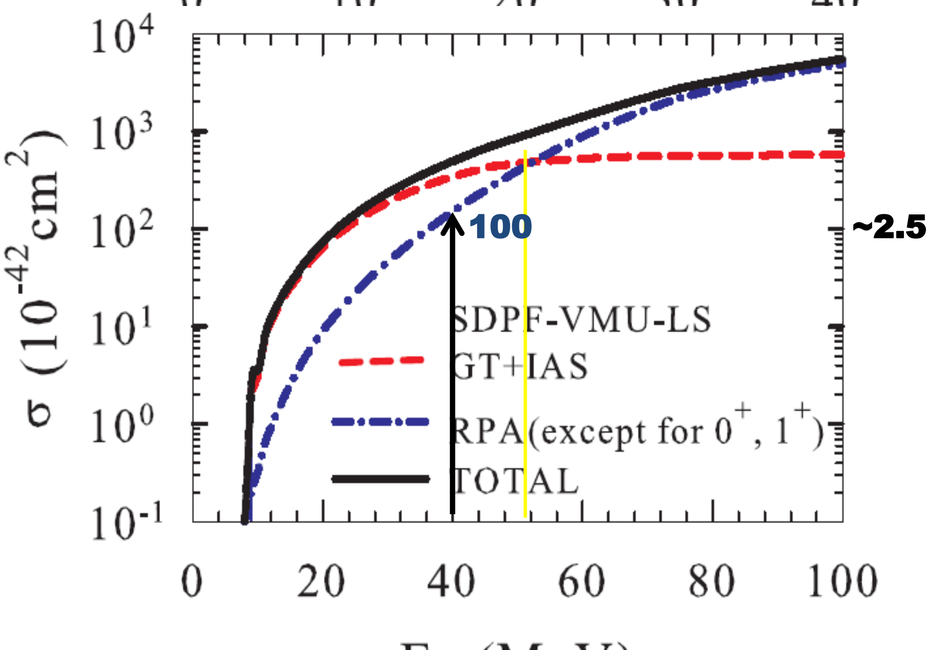

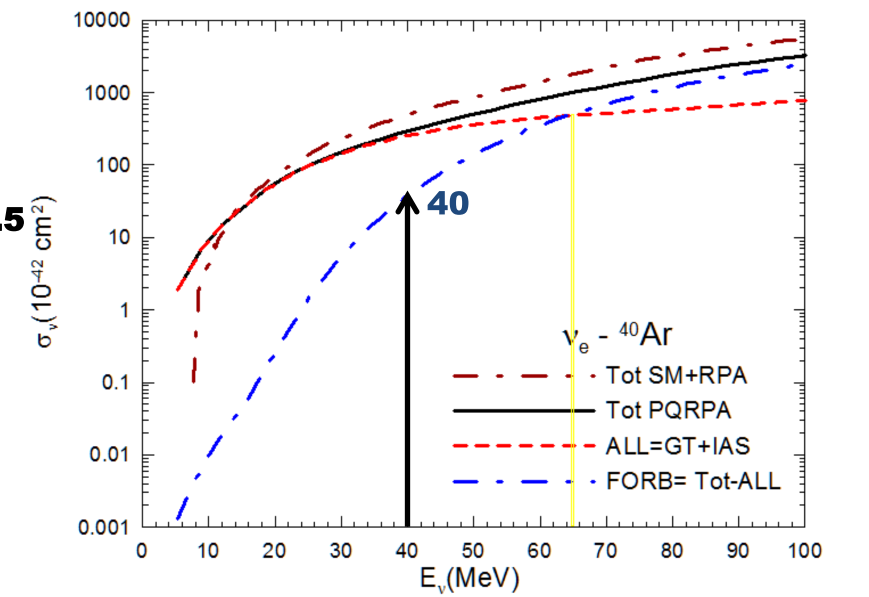

Neutrino/antineutrino cross sections ^{40}Ar

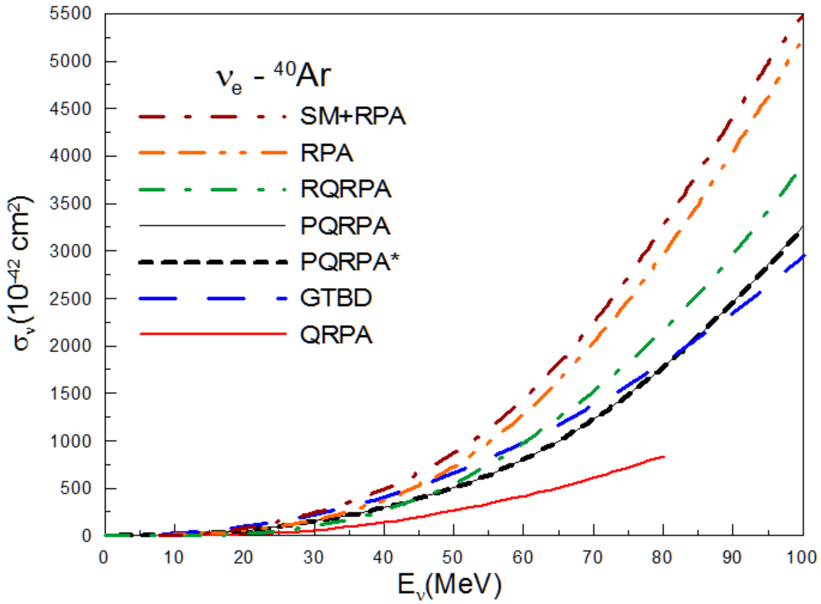

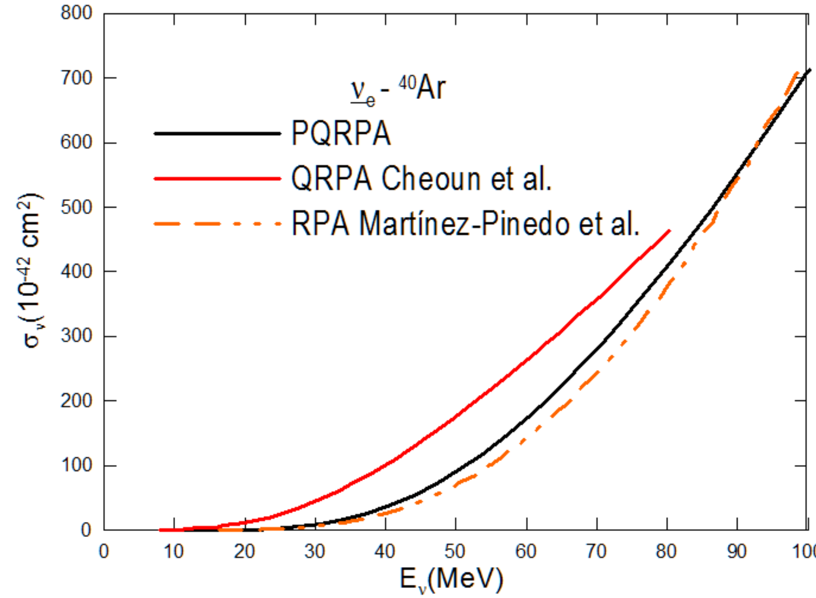

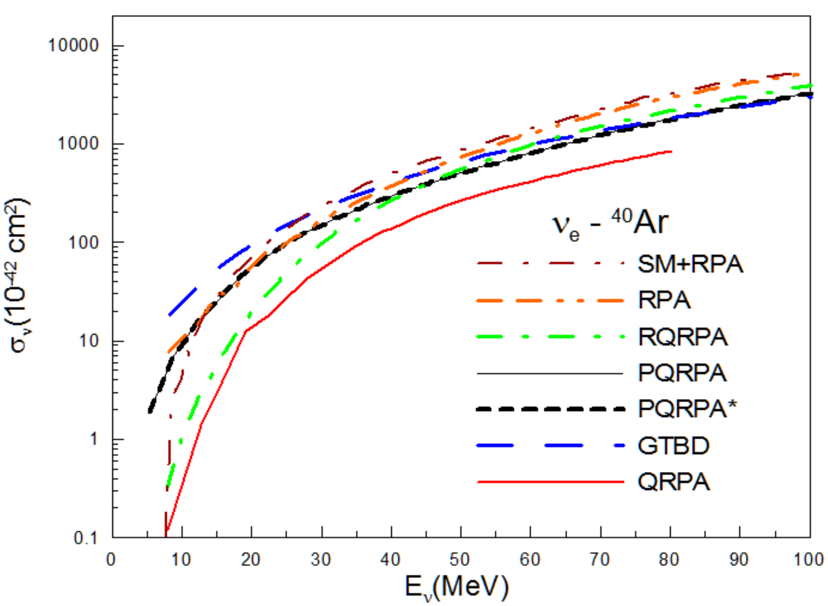

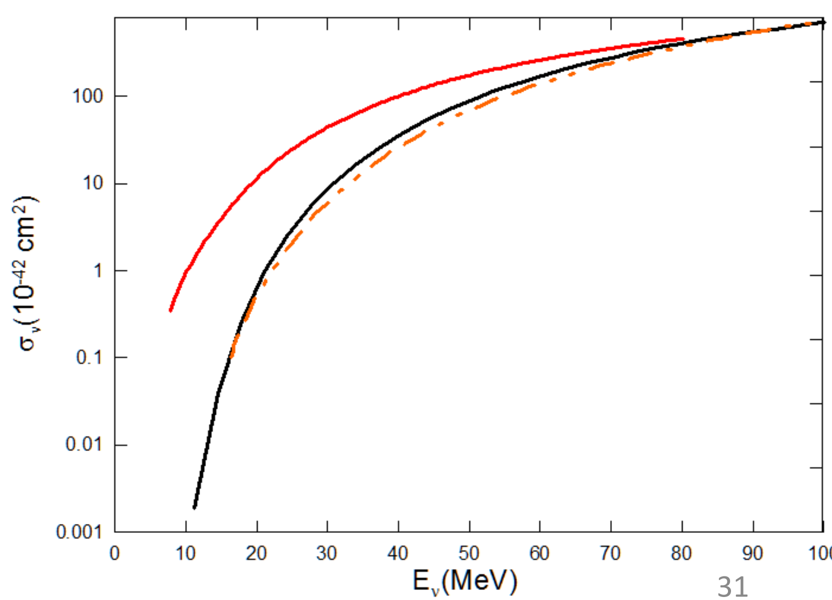

Neutrino/antineutrino cross sections ^{40}Ar

Folded cross section with SN fluxes

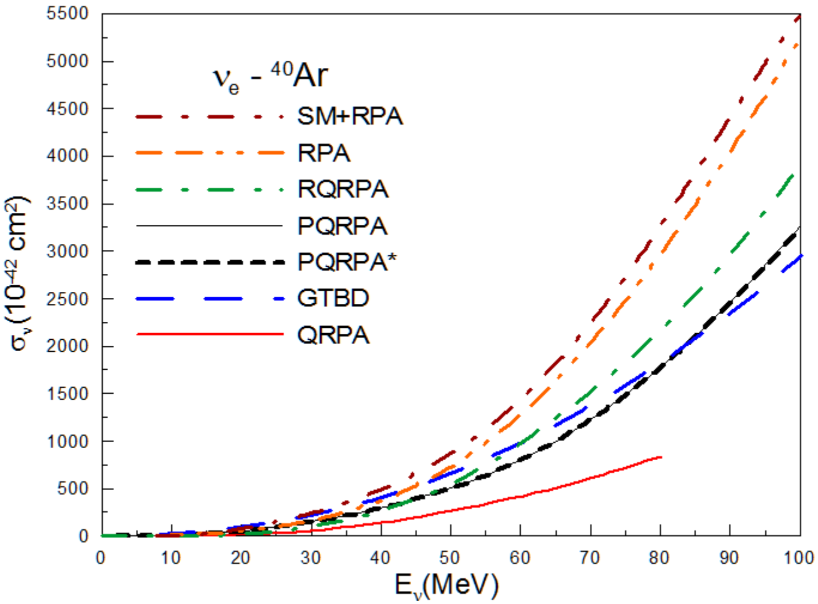

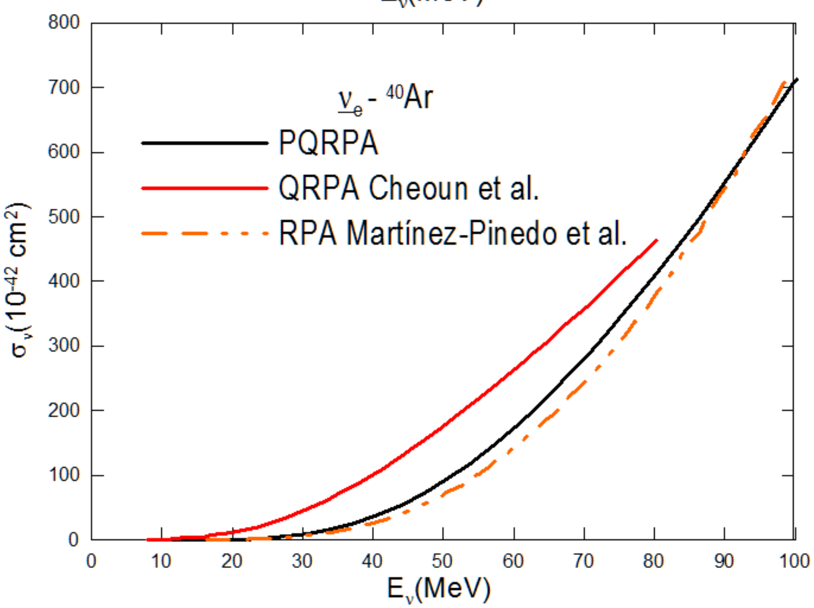

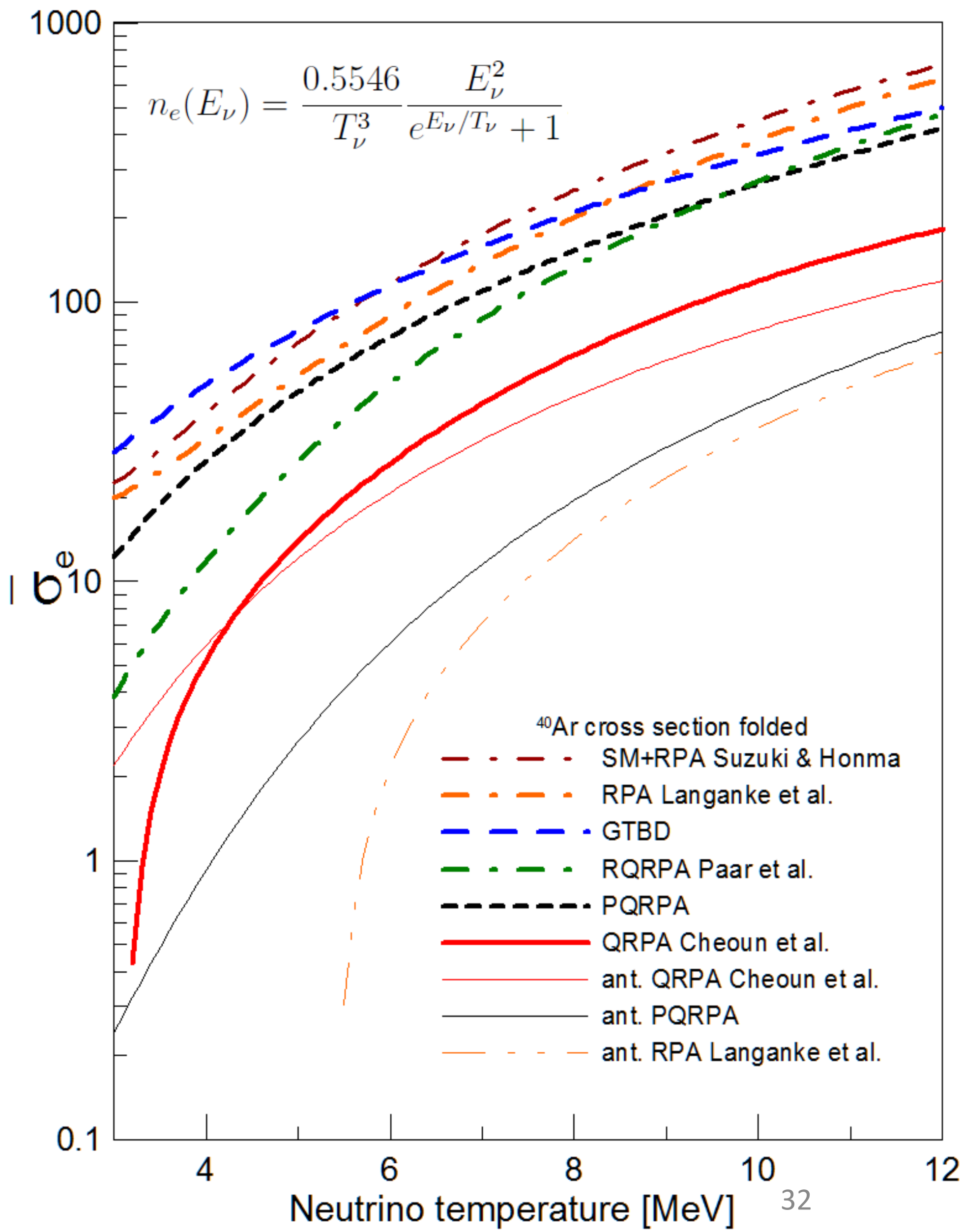

Summary

- All the formalism to describe weak-nuclear interaction present in the literature are equivalents!

(i)O'Connell, Donelly & Walecka, PR6,719 (1972)
(ii) Kuramoto etal. NPA 512, 711 (1990), up to $(|k|/M)^3$
(iii) Luyten etal. NP41,236 (1963),
(iv) Krmpotic etal. PRC71, 044319 (2005)

QRPA-type Models

disadvantages: Low energy neutrino regions up to 250 MeV, Skyrme interaction not good enough to make decisive improvement, Gogny interaction to check Skyrme, spherical nuclei, few QRPA model to non-spherical nuclei
advantages: self-consistency, large space, excellent agreement with exclusive reaction as well as SM, well description inclusive reaction and it´s possible describe up to 600 MeV neutrino energy with RQRPA, good option for astrophysical systematic calculations , main tool for 2 beta decay in the last 30 years
improvements:
through the Universal Nuclear Density Functional –UNEDF, non-spherical nuclei,

Large Scale Shell Model

disadvantages: only magic nuclei (N=50, 82, 126); only GT-decay; only spherical, great computational task, some cut due to a big configurational space sometimes this could be dangerous
advantages: several essential correlations included; treatment of even and odd isotopes.
improvements: Ab-initio shell model, new advances in nuclei as 12C,16O and 48Ca

Summary

- Due the universality of the weak hamiltonian, the nuclear models could be describe reasonably good the weak processes: GT strengths for β+ and β- (low energy region up to 40 MeV) and the inclusive muon capture rates (up to 100 MeV).
- A fine tunning requieres agreements with exclusive reactions, as such as exclusive muon capture rates to first lowest states. Scarce data available. Not for 40Ar.
- There is another possibility to obtain information about the allowed and forbidden states, these are the beta-beam experiments proposed by Lazauskus& Volpe and Balantekin.
- There are several parameters in the nuclear model, one of the most more important is $\mathbf{g_A}$ that goes from 1 to 1.27, leaving an averaged error up to 20 % in the GT-NME or CS.
- Some years ago G. McLaughlin talk me about to make a "gross averaged" of the CS for several nuclear models in 56Fe. I disagree in that moment, nevertheless I change of idea due the difficult to obtain an error in the nuclear models.
- In LArTPC detectors the most relevant cross is CC 40Ar(ν_e,e-)40K that has never been measured experimentally, but is was proposed by F. Cavana in NUINT 12 to be performed in NuSNS.

P. Möller
"…there is no "**correct**" model in nuclear physics. Any modeling of nuclear-structure properties involves approximations … to obtain a formulation that can be solved…, but that "**retains the essential features**" of the true system."